

# Efficient Temporal Pattern Mining in Big Time Series Using Mutual Information

Van Long Ho\*, Nguyen Ho\*, Torben Bach Pedersen\*  
Department of Computer Science, Aalborg University, Denmark  
\*{vlh, ntth, tbp}@cs.aau.dk

**Abstract**—Very large time series are increasingly available from an ever wider range of IoT-enabled sensors deployed in different environments. Significant insights can be obtained through mining temporal patterns from these time series. Unlike traditional pattern mining, temporal pattern mining (TPM) adds additional temporal aspect into extracted patterns, thus making them more expressive. However, adding the temporal dimension into patterns results in an exponential growth of the search space, significantly increasing the mining process complexity. Current TPM approaches either cannot scale to large datasets, or typically work on pre-processed event sequences rather than directly on time series. This paper presents our comprehensive Frequent Temporal Pattern Mining from Time Series (FTPMfTS) approach which provides the following contributions: (1) The end-to-end FTPMfTS process that directly takes time series as input and produces frequent temporal patterns as output. (2) The efficient Hierarchical Temporal Pattern Graph Mining (HTPGM) algorithm that uses efficient data structures to enable fast computations for support and confidence. (3) A number of pruning techniques for HTPGM that yield significantly faster mining. (4) An approximate version of HTPGM which relies on mutual information to prune unpromising time series, and thus significantly reduce the search space. (5) An extensive experimental evaluation on real-world datasets from the energy and smart city domains which shows that HTPGM outperforms the baselines and can scale to large datasets. The approximate HTPGM achieves up to 3 orders of magnitude speedup compared to the baselines and consumes significantly less memory, while obtaining high accuracy compared to the exact HTPGM.

## I. INTRODUCTION

Rapid advancements in IoT technology have enabled the collection of enormous amounts of time series at unprecedented scale and speed. For example, modern residential households are now equipped with smart meters and smart plugs, enabling fine-grained monitoring of the energy consumption of electrical appliances, or weather stations can have thousands of sensors to monitor hundreds of different variables related to weather conditions, generating terabytes of data everyday. Analyzing these massive, heterogeneous and rich time series can help uncover hidden patterns and extract new insights to support decision making and optimization.

As an example, consider Fig. 1 that shows the energy consumption time series of electrical appliances in a residential household. Such time series can be analyzed to identify how residents are interacting with electrical appliances in order to understand their living habits. For instance, a pattern of activations between Kitchen, Toaster and Microwave can be identified in Fig. 1, which shows that these devices are often used together, usually in the early morning and evening. Such

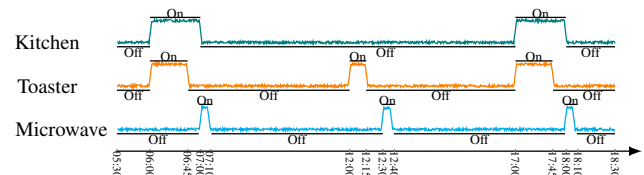


Fig. 1: Energy consumption time series of electrical appliances

insights are important, as they can be used to enable the building of smart houses, and/or optimize residential energy usage. For example, knowing that a resident always showers at 6:00 would enable pre-heating of hot water, e.g., when surplus wind energy is available.

Extracting such patterns is the task of pattern mining, an important branch in data mining. However, traditional pattern mining methods do not fully capture the temporal dimension. For example, sequential pattern mining would express the relation between appliances in Fig. 1 as  $\{Kitchen\ On\} \Rightarrow \{Toaster\ On, Microwave\ On\}$ , indicating that the occurrence of  $\{Toaster\ On, Microwave\ On\}$  is associated with the occurrence of  $\{Kitchen\ On\}$ . Such expressions omit the pattern occurrence times, and thus, leave out important information.

To overcome this limitation, a recent trend in pattern mining is to add temporal aspects into extracted patterns, forming a group of methods called *temporal pattern mining* (TPM). Using TPM, the previous pattern can be expressed as:  $[06:00,07:00] Kitchen\ On \Rightarrow [06:01,06:45] Toaster\ On \Rightarrow [07:00,07:10] Microwave\ On$ , or  $[1\ hour] Kitchen\ On \Rightarrow_{\text{after } 1\ min} [44\ minutes] Toaster\ On \Rightarrow_{\text{after } 15\ min} [10\ minutes] Microwave\ On$ . This type of patterns provides further details on when the relations between events happen, and for how long, making temporal patterns more expressive.

Although temporal patterns are useful, mining them is much more expensive than sequential patterns. Not only does the temporal information add extra computation to the mining process, the complex relations between events also result in an exponential growth of the search space, thus, significantly increases the mining process complexity. Current existing works such as [7, 20, 21], have tried to either use different representations such as augmented hierarchical representation to reduce the relation complexity, or propose different optimizations to improve TPM performance. However, these existing methods do not scale on big datasets as the challenge of the exponential search space still exists. Moreover, the methods do not work directly on time series, but rather on pre-processed event sequences.

*Contributions.* In the present paper, we present a comprehensive Frequent Temporal Pattern Mining from Time Series (FTPMfTS) approach to overcome the above limitations. Our solution provides the following key contributions. (1) We present the first end-to-end FTPMfTS process that receives a set of time series as input, and produces frequent temporal patterns as output. Within this process, a splitting strategy is proposed to convert time series into event sequences while ensuring the preservation of temporal patterns. (2) We provide a definition of temporal patterns through event instances, and thus, providing a more precise representation of the relations between events. Moreover, while adopting Allen relation model to represent relations between events, we simplify them, and propose to a buffer  $\epsilon$  in order to solve the exact time mapping problem while ensuring the mutually exclusive property of temporal relations. (3) We propose an efficient Hierarchical Temporal Pattern Graph Mining (HTPGM) method to efficiently mine frequent temporal patterns. HTPGM has several important novelties. First, HTPGM employs efficient data structures, Hierarchical Pattern Graph and *bitmap*, to enable fast computations for support and confidence of temporal patterns. Second, two groups of pruning techniques based on the Apriori principle and the transitivity property of temporal relations are introduced in HTPGM to enable faster mining. (4) Based on mutual information, we propose an approximate version of HTPGM that can prune unpromising time series, and thus, significantly reduces the search space. This approximation allows HTPGM scale on big datasets. (5) We perform an extensive experimental evaluation on real-world datasets which shows that HTPGM outperforms the baselines and can scale to large datasets. The approximate HTPGM can achieve up to 3 orders of magnitude speedup and consumes significantly less memory, while obtaining high accuracy compared to the exact HTPGM.

*Paper outline.* Section II covers related work. Section III presents related concepts and defines the problem. Sections IV and V present the exact and approximate mining methods. Section VI shows experimental evaluation and Section VII concludes the paper.

## II. RELATED WORK

*Temporal pattern mining:* Compare to sequential pattern mining, there are fewer works that investigate the temporal pattern mining problem. One of the first works in this area is the proposal of Kam et al. [14] that uses a hierarchical representation to manage temporal relations, and based on that to mine temporal patterns. This approach however suffers from ambiguity when presenting temporal relations. To overcome this, Wu et al. [22] define new non-ambiguous temporal relations, and develop a method called TPprefix to mine temporal patterns. TPprefix however has several inherent limitations: it scans the database repeatedly, and the algorithm does not employ any pruning strategies to reduce the search space. In [18], Moskovitch et. al. design a TPM algorithm using the transitivity property of temporal relations. They use this property to generate candidates through inferring new relations

between events. This differs from HTPGM as we use this transitivity property for pruning. In [3], Iyad et. al. rely on a temporal pattern mining framework to detect events in time series. Their focus however is to find irregularities in the data.

Other approaches, such as Nguyen et al. [19] propose to mine temporal rules on cancer treatment data, Iyad et al. [4] propose a TPM algorithm to classify health record data, Campbell et al. [6] introduce a temporal condition pattern mining method to characterize pediatric asthma. However, these approaches are very domain-specific, and thus cannot generalize to other domains.

Among the existing TPM methods, H-DFS [20], TPMiner [7], and IEMiner [21] are the most well-known. In [20], Papapetrou et al. propose a hybrid algorithm called H-DFS using both bread-first and depth-first search strategies to mine frequent arrangements of temporal intervals. H-DFS first transforms an event sequence into a vertical representation using id-lists. Then, the id-list of one event is merged with the id-list of other events to generate temporal patterns. This approach however does not scale well when the temporal pattern length increases. In [7], Chen et al. design TPMiner to mine temporal patterns. They propose endpoint and endtime representations to simplify the complex relations among events. Similar to [20], TPMiner does not scale when the data size increases. In [21], Patel et al. design a hierarchical lossless representation to model relations between events, and propose an efficient algorithm called IEMiner to mine patterns from interval-based events. IEMiner uses Apriori-based optimizations to reduce the search space. From our experiments, IEMiner achieves the best performance among these three methods.

*Using correlations in temporal pattern mining:* There have been a few attempts to apply different correlation measures such as expected support [1], all-confidence [17], mutual information [5, 10, 15, 23] to optimize the pattern mining process. However, these attempts are only on sequential pattern mining. There are not any works that tries to incorporate correlation measures to TPM problem.

## III. PRELIMINARIES

In this section, we introduce the notations and the main concepts that will be used throughout the paper.

### A. Temporal Event of Time Series

**Definition 3.1** (Time series) A *time series*  $X = x_1, x_2, \dots, x_n$  is a sequence of data values that measure the same phenomenon during an observation time period, and are chronologically ordered.

**Definition 3.2** (Symbolic representation of a time series) A *symbolic representation*  $\mathcal{X}_S$  of a time series  $X$  encodes the raw values of  $X$  to a sequence of symbols. A finite set of permitted symbols used to encode  $X$  is called the *symbol alphabet* of  $X$ , denoted as  $\Sigma_X$ .

The symbolic representation of a time series  $X$  can be easily obtained by using a mapping function  $f : X \rightarrow \Sigma_X$  that maps each value  $x_i \in X$  to a symbol  $\omega \in \Sigma_X$ .

As an example, assume  $X = 1.61, 2.95, 1.21, 0.41, 0.05, 0.0$  is a time series representing the energy consumption of an electrical device. Then, using the symbol alphabet  $\Sigma_X = \{\text{On}, \text{Off}\}$ , where On represents the device is on and operating (e.g., when  $x_i \geq 0.5$ ), and Off represents the device is off (when  $x_i < 0.5$ ), we can obtain the symbolic representation of  $X$  as:  $\mathcal{X}_S = \text{On}, \text{On}, \text{On}, \text{Off}, \text{Off}, \text{Off}$ .

**Definition 3.3** (Symbolic database) Given a set of time series  $\mathcal{X} = \{X_1, \dots, X_n\}$ , the collection of symbolic representations of the time series in  $\mathcal{X}$  forms a *symbolic database*  $\mathcal{D}_{\text{SYB}}$ .

Table I is an example of a symbolic database  $\mathcal{D}_{\text{SYB}}$ . Here, we have a set of six time series representing the energy consumption of six electrical appliances: {Kitchen, Toaster, Microwave, Coffee machine, Clothes Ironer, and Blender}. For brevity, we name the appliances as {K, T, M, C, I, B}, respectively. In this specific example, all appliances have the same symbol alphabet  $\Sigma = \{\text{On}, \text{Off}\}$ , and the symbolic database  $\mathcal{D}_{\text{SYB}}$  is obtained by transforming each time series into a sequence of symbols, as in Table I.

**Definition 3.4** (Temporal event of a time series) A *temporal event*  $E$  of a time series  $X$  is a tuple  $E = (\omega, T)$  where  $\omega \in \Sigma_X$  is a symbol, and  $T = \{[t_{s_i}, t_{e_i}]\}$  is a set of time intervals during which  $X$  is associated with the symbol  $\omega$ .

Intuitively, a temporal event represents a state of the time series  $X$  occurring during the recorded time intervals. For example, if  $X$  is the energy consumption of the Kitchen,  $X$  can have a temporal event representing the state “Kitchen is On” during certain time intervals.

Given a symbolic representation of a time series  $X$ , a temporal event of  $X$  is formed by combining identical consecutive symbols of  $X$  into one time interval. For example, consider the symbolic representation of  $K$  in Table I. We can combine its consecutive On symbols to form the temporal event “Kitchen is On” as: (KOn,  $\{[10:00, 10:15], [10:35, 10:40], [11:15, 11:25], [11:50, 12:00], [12:15, 12:20], [12:35, 12:45]\}$ ).

**Definition 3.5** (Instance of a temporal event) Let  $E = (\omega, T)$  be a temporal event, and  $[t_{s_i}, t_{e_i}] \in T$  be a time interval. The tuple  $e = (\omega, [t_{s_i}, t_{e_i}])$  is called an *instance* of the event  $E$ , representing a single occurrence of  $E$  during  $[t_{s_i}, t_{e_i}]$ . We use  $E_{\triangleright e}$  to denote that event  $E$  has an instance  $e$ .

### B. Relations between Temporal Events

To find temporal patterns, we need to define the relations between temporal events. In the present paper, we adopt a popular relation model proposed by Allen [2] to represent relations between temporal events. However, we simplify Allen’s relations, reducing the 7 original relations into 3 basic ones, while still maintaining a similar expressive power. Moreover, to avoid the exact time mapping problem in Allen model, we adopt the buffer idea in [?] that adds a *buffer*  $\epsilon$  to the relation’s endpoints as a tolerant duration. However, we change the way  $\epsilon$  is used to ensure that relations are mutually exclusive. The definitions of temporal relations are provided below.

Consider two temporal events  $E_1$  and  $E_2$ , and their corresponding instances,  $e_1$  occurring during  $[t_{s_1}, t_{e_1}]$  and  $e_2$  occurring during  $[t_{s_2}, t_{e_2}]$ . Let  $\epsilon$  be a non-negative number

( $\epsilon \geq 0$ ) representing the buffer value. The following relations can be defined between  $E_1$  and  $E_2$  through  $e_1$  and  $e_2$ .

**Definition 3.6** (Follow) Two temporal events  $E_1$  and  $E_2$  form a *Follow* relation through  $e_1$  and  $e_2$ , denoted as Follows( $E_{1_{\triangleright e_1}}, E_{2_{\triangleright e_2}}$ ) or  $E_{1_{\triangleright e_1}} \rightarrow E_{2_{\triangleright e_2}}$ , iff  $t_{e_1} \pm \epsilon \leq t_{s_2}$ .

**Definition 3.7** (Contain) Two temporal events  $E_1$  and  $E_2$  form a *Contain* relation through  $e_1$  and  $e_2$ , denoted as Contains( $E_{1_{\triangleright e_1}}, E_{2_{\triangleright e_2}}$ ) or  $E_{1_{\triangleright e_1}} \succcurlyeq E_{2_{\triangleright e_2}}$ , iff  $(t_{s_1} \leq t_{s_2}) \wedge (t_{e_1} \pm \epsilon \geq t_{e_2})$ .

**Definition 3.8** (Overlap) Two temporal events  $E_1$  and  $E_2$  form an *Overlap* relation through  $e_1$  and  $e_2$ , denoted as Overlaps( $E_{1_{\triangleright e_1}}, E_{2_{\triangleright e_2}}$ ) or  $E_{1_{\triangleright e_1}} \bowtie E_{2_{\triangleright e_2}}$ , iff  $(t_{s_1} < t_{s_2}) \wedge (t_{e_1} \pm \epsilon < t_{e_2}) \wedge (t_{e_1} - t_{s_2} \geq d_o \pm \epsilon)$ , where  $d_o$  is a positive number representing the minimal overlapping duration between two event instances:  $0 \leq \epsilon \ll d_o$ .

Table II illustrates the three temporal relations and their conditions. Note that since relations between temporal events are formed through their instances, it is possible that the same pair of events forms different relations through different instances, or an event can form the relation with itself. In this case, we call it a *self-relation*.

### C. Temporal Pattern

**Definition 3.9** (Temporal sequence) A list of event instances  $S = \langle e_1, \dots, e_i, \dots, e_n \rangle$  forms a *temporal sequence* if the event instances are chronologically ordered by their start times. Moreover,  $S$  has size  $n$ , denoted as  $|S| = n$ .

**Definition 3.10** (Temporal sequence database) A collection of temporal sequences forms a *temporal sequence database*  $\mathcal{D}_{\text{SEQ}}$  where each row  $i$  contains a temporal sequence  $S_i$ .

Table III is an example of temporal sequence database  $\mathcal{D}_{\text{SEQ}}$ , created from the symbolic database  $\mathcal{D}_{\text{SYB}}$  in Table I.

**Definition 3.11** (Temporal pattern) Let  $\mathfrak{R} = \{\text{Follow}, \text{Contain}, \text{Overlap}\}$  be the set of relations between temporal events. A *temporal pattern*  $P = \langle (E_1, r_{12}, E_2), \dots, (E_i, r_{ij}, E_j), \dots, (E_{n-1}, r_{(n-1)(n)}, E_n) \rangle$  is a list of triples where each triple represents a relation between two events. In the triple  $(E_i, r_{ij}, E_j)$ ,  $r_{ij} \in \mathfrak{R}$  is a temporal relation, and  $E_i, E_j$  are temporal events.

A temporal pattern that has  $n$  events is called an  $n$ -event pattern. For the notation, we use  $E_i \in P$  to denote that the event  $E_i$  occurs in  $P$ , and  $P_1 \subseteq P$  to say that the temporal pattern  $P_1$  is a sub-pattern of  $P$ .

**Definition 3.12** (Temporal sequence supports a temporal pattern) Let  $S = \langle e_1, \dots, e_i, \dots, e_n \rangle$  be a temporal sequence. We say that  $S$  supports a temporal pattern  $P$ , denoted as  $P \in S$ , iff  $|S| \geq 2 \wedge \forall (E_i, r_{ij}, E_j) \in P, \exists (e_l, e_m) \in S$  such that  $r_{ij}$  holds between  $E_{i_{\triangleright e_l}}$  and  $E_{j_{\triangleright e_m}}$ .

If a pattern  $P$  is supported by a sequence  $S = \langle e_1, \dots, e_i, \dots, e_n \rangle$ , then  $P$  can be written in the form  $P = \langle (E_{1_{\triangleright e_1}}, r_{12}, E_{2_{\triangleright e_2}}), \dots, (E_{n-1_{\triangleright e_{n-1}}}, r_{(n-1)(n)}, E_{n_{\triangleright e_n}}) \rangle$ , where the relation between events in each triple is expressed using the event instances.

In Fig. 1, the temporal sequence  $S = \langle (\text{KOn}, [06:00, 07:00]), (\text{TOn}, [06:00, 06:15]), (\text{MOn}, [06:15, 06:30]) \rangle$  represents a chronological order of appliances’ activations in a

TABLE I: A symbolic database  $\mathcal{D}_{\text{SYB}}$ 

Time	10:00	10:05	10:10	10:15	10:20	10:25	10:30	10:35	10:40	10:45	10:50	10:55	11:00	11:05	11:10	11:15	11:20	11:25	11:30	11:35	11:40	11:45	11:50	11:55	12:00	12:05	12:10	12:15	12:20	12:25	12:30	12:35	12:40	12:45	12:50	12:55
K	On	On	On	On	Off	Off	Off	On	On	Off	Off	Off	Off	Off	On	On	On	Off	Off	Off	Off	On	On	On	Off	Off	On	On	Off	Off	On	On	On	Off	Off	
T	Off	On	On	On	Off	Off	Off	On	On	Off	Off	On	On	Off	Off	On	On	On	Off	Off	Off	Off	On	On	On	Off	Off	On	On	Off	Off	Off	On	On	On	Off
M	Off	Off	Off	Off	On	On	On	Off	Off	On	On	On	Off	On	On	Off	Off	Off	On	On	Off	On	On	Off	Off	On	On	Off	Off	On	On	On	Off	Off	On	On
c	Off	Off	Off	Off	On	On	On	Off	Off	On	On	Off	On	On	On	Off	Off	Off	On	On	Off	On	On	Off	Off	On	On	Off	Off	On	On	On	Off	Off	On	On
I	Off	On	On	Off	On	On	Off	Off	Off	Off	Off	On	On	Off																						
B	Off	On	On	Off	On	On	Off	Off	Off	Off	Off	Off	On	On	Off	Off	Off	Off	Off	Off	On	On														

TABLE II: Temporal relations between events

Follow relation: $E_{1 \triangleright e_1} \rightarrow E_{2 \triangleright e_2}$	$t_{e_1} \pm \epsilon \leq t_{s_2}$
Contain relation: $E_{1 \triangleright e_1} \supseteq E_{2 \triangleright e_2}$	$(t_{s_1} \leq t_{s_2}) \wedge (t_{e_1} \pm \epsilon \geq t_{e_2})$
Overlap relation: $E_{1 \triangleright e_1} \cap E_{2 \triangleright e_2}$	$(t_{s_1} < t_{s_2}) \wedge (t_{e_1} \pm \epsilon < t_{e_2}) \wedge (t_{e_1} - t_{s_2} \geq d_o \pm \epsilon)$

 TABLE III: A temporal sequence database  $\mathcal{D}_{\text{SEQ}}$ 

ID	Temporal sequences
1	(KOn,[10:00,10:15]), (KOff,[10:15,10:35]), (KOn,[10:35,10:40]), (TOff,[10:00,10:05]), (TON,[10:05,10:15]), (TOff,[10:15,10:35]), (TON,[10:35,10:40]), (MOff,[10:00,10:20]), (MON,[10:20,10:30]), (MOff,[10:30,10:40]), (COff,[10:00,10:20]), (CON,[10:20,10:30]), (COff,[10:30,10:40]), (IOff,[10:00,10:40]), (BOff,[10:00,10:35]), (BON,[10:35,10:40])
2	(KOff,[10:45,11:15]), (KOn,[11:15,11:25]), (TOff,[10:45,10:55]), (TON,[10:55,11:00]), (TOff,[11:00,11:15]), (TON,[11:15,11:25]), (MON,[10:45,10:55]), (MOff,[10:55,11:05]), (MON,[11:05,11:10]), (MOff,[11:10,11:25]), (CON,[10:45,10:50]), (COff,[10:50,11:00]), (CON,[11:00,11:10]), (COff,[11:10,11:25]), (ION,[10:45,10:50]), (IOff,[10:50,11:20]), (ION,[11:20,11:25]), (BOff,[10:45,11:25])
3	(KOff,[11:30,11:50]), (KOn,[11:50,12:00]), (KOff,[12:00,12:10]), (TOff,[11:30,11:50]), (TON,[11:50,12:00]), (TOff,[12:00,12:10]), (MON,[11:30,11:35]), (MOff,[11:35,11:45]), (MON,[11:45,11:50]), (MOff,[11:50,12:05]), (MON,[12:05,12:10]), (CON,[11:30,11:35]), (COff,[11:35,11:45]), (CON,[11:45,11:50]), (COff,[11:50,12:05]), (COff,[11:50,12:10]), (ION,[11:30,12:10]), (BON,[11:30,11:35]), (BOff,[11:35,12:10])
4	(KOn,[12:15,12:20]), (KOff,[12:20,12:35]), (KOn,[12:35,12:45]), (KOff,[12:45,12:55]), (TON,[12:15,12:20]), (TOff,[12:20,12:40]), (TON,[12:40,12:50]), (TOff,[12:50,12:55]), (MOff,[12:15,12:25]), (MON,[12:25,12:35]), (MOff,[12:35,12:50]), (MON,[12:50,12:55]), (COff,[12:15,12:25]), (CON,[12:25,12:35]), (COff,[12:35,12:50]), (CON,[12:50,12:55]), (ION,[12:15,12:20]), (IOff,[12:20,12:40]), (ION,[12:40,12:45]), (IOff,[12:45,12:55]), (BON,[12:15,12:20]), (BOff,[12:20,12:50]), (BON,[12:50,12:55])

household. The sequence  $S$  supports a 3-event pattern where the relations between each pair of events are: Contain(KOn, TOn), Contain(KOn, MOn), Follow(TOn, MOn).

*Constraint on maximal duration of a pattern:* Let  $P \in S$  be a temporal pattern formed by the sequence  $S$ . The duration between the start time of the instance  $e_1$ , and the end time of the instance  $e_n$  in  $S$  must not exceed the predefined maximal time duration  $t_{\max}$ :  $t_{e_n} - t_{s_1} \leq t_{\max}$ .

The maximal duration constraint ensures that any two events of a temporal pattern are temporally related within a limited time. This guarantees that the formed relations are temporally valid, and thus, enables the pruning of invalid patterns. For example, under this constraint, a *Follow* relation between a “Kitchen is On” event and a “Microwave is On” event happened one year apart should be considered invalid.

#### D. Frequent Temporal Pattern

Given a temporal sequence database  $\mathcal{D}_{\text{SEQ}}$ , we want to find temporal patterns that occur frequently in  $\mathcal{D}_{\text{SEQ}}$ . We use *support* and *confidence* to measure the frequency of a pattern. **Definition 3.13** (Support of a temporal event) The *support* of a temporal event  $E$  in  $\mathcal{D}_{\text{SEQ}}$  is the number of temporal sequences  $S \in \mathcal{D}_{\text{SEQ}}$  that contain at least one instance of  $E$ .

$$\text{supp}(E) = |\{S \in \mathcal{D}_{\text{SEQ}} \text{ s.t. } \exists e \in S : E \triangleright e\}| \quad (1)$$

The *relative support* of  $E$  is the fraction between  $\text{supp}(E)$  and the size of  $\mathcal{D}_{\text{SEQ}}$ :

$$\text{rel-supp}(E) = \text{supp}(E) / |\mathcal{D}_{\text{SEQ}}| \quad (2)$$

Similarly, the support of a group of two or more events  $(E_1, \dots, E_n)$ , denoted as  $\text{supp}(E_1, \dots, E_n)$ , is the number of

temporal sequences  $S \in \mathcal{D}_{\text{SEQ}}$  which contain at least one instance of the group.

**Definition 3.14** (Support of a temporal pattern) The *support* of a temporal pattern  $P$  is the number of temporal sequences  $S \in \mathcal{D}_{\text{SEQ}}$  that form  $P$ .

$$\text{supp}(P) = |\{S \in \mathcal{D}_{\text{SEQ}} \text{ s.t. } P \in S\}| \quad (3)$$

The *relative support* of  $P$  in  $\mathcal{D}_{\text{SEQ}}$  is the fraction between  $\text{supp}(P)$  and the size of  $\mathcal{D}_{\text{SEQ}}$ :

$$\text{rel-supp}(P) = \text{supp}(P) / |\mathcal{D}_{\text{SEQ}}| \quad (4)$$

**Definition 3.15** (Confidence of a pair of events) Let  $(E_i, E_j)$  be a pair of temporal events. The *confidence* of  $(E_i, E_j)$  in  $\mathcal{D}_{\text{SEQ}}$  is defined as

$$\text{conf}(E_i, E_j) = \frac{\text{supp}(E_i, E_j)}{\max\{\text{supp}(E_i), \text{supp}(E_j)\}} \quad (5)$$

**Definition 3.16** (Confidence of a temporal pattern) The *confidence* of a temporal pattern  $P$  in  $\mathcal{D}_{\text{SEQ}}$  is defined as

$$\text{conf}(P) = \frac{\text{supp}(P)}{\max_{1 \leq k \leq |P|} \{\text{supp}(E_k)\}} \quad (6)$$

where  $E_k \in P$  is a temporal event.

The denominator in Eq. (6) is the maximum support of the events in  $P$ . Thus, the confidence computed in Eq. (6) is the minimum confidence of a pattern  $P$  in  $\mathcal{D}_{\text{SEQ}}$ , representing how likely a pattern  $P$  (at least) is, given the occurrence of its most frequent event. We are now ready to define the problem of mining frequent temporal patterns from time series.

**Frequent Temporal Pattern Mining from Time Series (FTPMfTS):** Given a set of time series  $\mathcal{X} = \{X_1, \dots, X_n\}$ ,

let  $\mathcal{D}_{\text{SEQ}}$  be the temporal sequence database obtained from  $\mathcal{X}$ , and  $\sigma$  and  $\delta$  be the support and confidence thresholds, respectively. The FTPMfTS problem aims to find all temporal patterns  $P$  that have high enough support and confidence in  $\mathcal{D}_{\text{SEQ}}$ :  $\text{supp}(P) \geq \sigma \wedge \text{conf}(P) \geq \delta$ .

#### IV. FREQUENT TEMPORAL PATTERN MINING

##### A. Overview of the FTPMfTS Process

Fig. 2 depicts the overall FTPMfTS process to mine frequent patterns from a set of time series. The process consists of two phases. The first phase, *Data Transformation*, receives a set of time series  $\mathcal{X}$  as an input, and converts it into a symbolic database  $\mathcal{D}_{\text{SYB}}$  through the *Symbolic Time Series Representation* (Step 1a). Then,  $\mathcal{D}_{\text{SYB}}$  is converted into a temporal sequence database  $\mathcal{D}_{\text{SEQ}}$  through the *Temporal Sequence Database Conversion* (Step 1b). The second phase, *Frequent Temporal Pattern Mining*, mines frequent patterns from  $\mathcal{D}_{\text{SEQ}}$ . This goes through 3 steps: (Step 2a) *Frequent Single Event Mining*, (Step 2b) *Frequent 2-Event Pattern Mining*, and (Step 2c) *Frequent k-Event Pattern Mining* ( $k > 2$ ). The final output is a set of all frequent temporal patterns in  $\mathcal{D}_{\text{SEQ}}$ .

##### B. Data Transformation

1) *Symbolic Time Series Representation*: Given a set of time series  $\mathcal{X}$ , the symbolic representation of each time series  $X \in \mathcal{X}$  can be easily obtained by using a mapping function described in Def. 3.2, after which will form  $\mathcal{D}_{\text{SYB}}$ .

2) *Temporal Sequence Database Conversion*: To convert  $\mathcal{D}_{\text{SYB}}$  to  $\mathcal{D}_{\text{SEQ}}$ , a straightforward approach is to split the symbolic time series in  $\mathcal{D}_{\text{SYB}}$  into equal length temporal sequences, where each sequence belongs to one row in  $\mathcal{D}_{\text{SEQ}}$ . For example, consider Table I. If we decide to split each symbolic series in  $\mathcal{D}_{\text{SYB}}$  into 4 equal length temporal sequences, then each sequence will last for 40 minutes. The first sequence  $S_1$  will contain temporal events of  $K, T, M, C, I,$  and  $B$  from 10:00 to 10:40. The second sequence  $S_2$  contains temporal events from 10:45 to 11:25, and similarly for  $S_3$  and  $S_4$ .

However, this splitting can lead to a potential loss of temporal patterns. The loss happens when a *splitting point* accidentally divides a temporal pattern into different sub-patterns, and places them into separate sequences. We explain this situation in Fig. 3a, considering the two sequences  $S_1$  and  $S_2$ , each of length  $t$ . Here, the splitting point divides a pattern of 4 events,  $\{\text{KOn}, \text{TOn}, \text{MOn}, \text{COOn}\}$ , into two sub-patterns, in which  $\text{KOn}$  and  $\text{TOn}$  are placed in  $S_1$ , and  $\text{MOn}$  and  $\text{COOn}$  in  $S_2$ . This results in the loss of this 4-event pattern which can be identified only when all 4 events are in the same sequence.

To prevent the loss, we propose a *splitting strategy* using overlapping sequences. Specifically, two consecutive sequences are overlapped by a duration  $t_{\text{ov}}$  ( $0 \leq t_{\text{ov}} \leq t_{\text{max}}$ , where  $t_{\text{max}}$  is the *maximal duration* of a temporal pattern). The value of  $t_{\text{ov}}$  decides how large the overlap between  $S_i$  and  $S_{i+1}$  is:  $t_{\text{ov}} = 0$  results in no overlap, i.e., no redundancy, but with a potential loss of patterns, while  $t_{\text{ov}} = t_{\text{max}}$  creates large overlappings between sequences, i.e., high redundancy, but all patterns can be preserved. As illustrated in Fig. 3b, the

overlapping between  $S_1$  and  $S_2$  keeps the 4 events together in the same sequence  $S_2$ , and thus, helps preserve the pattern.

##### C. Frequent Temporal Patterns Mining

We now present our efficient mining method, called Hierarchical Temporal Pattern Graph Mining (HTPGM), to mine frequent temporal patterns from  $\mathcal{D}_{\text{SEQ}}$ . The main novelties of HTPGM lie in: a) the use of efficient data structures, i.e., the Hierarchical Pattern Graph and *bitmap indexing*, to enable fast computations for support and confidence, and b) the proposal of three different pruning techniques to optimize the mining process. These pruning techniques are based on: the Apriori principle and the temporal transitivity property of temporal events. Later in Section V, we introduce an additional pruning technique that is based on mutual information and is built on top of HTPGM to further optimize the mining process. We now discuss the efficient data structures used in our method.

*Hierarchical Pattern Graph (HPG)*: We use a hierarchical graph structure, called the *Hierarchical Pattern Graph*, to keep track of the frequent events and patterns found in each mining step. This graph structure allows HTPGM to mine iteratively (e.g., 2-event patterns are mined based on frequent single events, 3-event patterns are mined based on 2-event patterns, and so on), and also to do effective pruning. Fig. 4 shows the HPG built from  $\mathcal{D}_{\text{SEQ}}$  in Table III. The root of the graph is an empty set  $\emptyset$ , and each level  $L_k$  maintains frequent  $k$ -event patterns. As HTPGM proceeds, HPG is constructed gradually. We will explain this process in each following mining step.

*Efficient bitmap indexing*: We use *bitmap* to index the occurrences of events and patterns in  $\mathcal{D}_{\text{SEQ}}$ , enabling fast computations for support and confidence. Specifically, each event  $E$  or pattern  $P$  found in  $\mathcal{D}_{\text{SEQ}}$  is associated with a *bitmap* that indicates where  $E$  or  $P$  has occurred. Each *bitmap*  $b$  has length  $|\mathcal{D}_{\text{SEQ}}|$  (i.e., the number of sequences), and has value  $b[i] = 1$  if  $E$  or  $P$  is present in sequence  $i$  of  $\mathcal{D}_{\text{SEQ}}$ , or  $b_E[i] = 0$  otherwise. Constructing the *bitmap* is also done step by step. For single events in  $\mathcal{D}_{\text{SEQ}}$ , *bitmaps* are built by scanning  $\mathcal{D}_{\text{SEQ}}$  only once. Fig. 4 shows an example of *bitmap*. At level  $L_1$ , the event  $\text{KOn}$  has the *bitmap*  $b_{\text{KOn}} = [1, 1, 1, 1]$ , indicating that  $\text{KOn}$  occurs in all sequences of  $\mathcal{D}_{\text{SEQ}}$ .

##### D. Mining Frequent Single Events

The first step in HTPGM is to find frequent single events. This can easily be done using the created *bitmap*. For each event  $E_i$  in  $\mathcal{D}_{\text{SEQ}}$ , its support  $\text{supp}(E_i)$  is computed by counting the number of set bits in *bitmap*  $b_{E_i}$ , and comparing  $\text{supp}(E_i)$  to the threshold  $\sigma$ . Note that for single events, *confidence* is not considered since it is always 1.

*Complexity*: The complexity of finding frequent single events in  $\mathcal{D}_{\text{SEQ}}$  is  $O(m \cdot |\mathcal{D}_{\text{SEQ}}|)$ , where  $m$  is the number of distinct events.

*Proof*. Detail proofs of the complexities, lemmas and theorems in this article can be found in the technical report [13].  $\square$

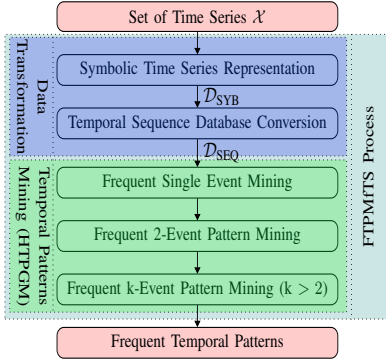


Fig. 2: FTPMfTS process

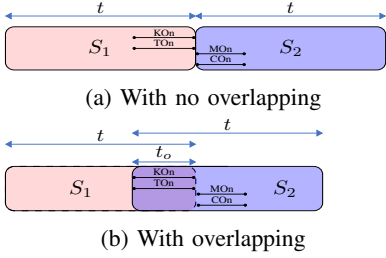


Fig. 3: Splitting strategy

After the frequent single events are found, HTPGM builds the first level  $L_1$  of HPG. We illustrate this process using Table III, with  $\sigma = 0.7$  and  $\delta = 0.7$ . Here, after the first mining step, the event  $IO_n$  becomes infrequent since it only appears in sequences 2 and 4, and thus, is not selected. Instead, other events are frequent and thus, are selected to form the set  $IFreq$  which then is used to build level  $L_1$  in HPG. In  $L_1$ , each node represents one frequent single event. The data structure of each node contains a unique event name, a *bitmap*, and a list of event instances and their corresponding time intervals (see for example event  $KO_n$  at  $L_1$  in Fig. 4).

### E. Mining Frequent 2-event Patterns

1) *Search space of FTPMfTS*: The second step in HTPGM is to find frequent 2-event temporal patterns. A straightforward approach would be to enumerate all possible pairs of events, and check whether each event pair can form frequent patterns. However, this *naive* approach is very expensive. Not only does it need to repeatedly scan  $D_{SEQ}$  to check for each combination of events, the complex relations between events also result in an exponential growth of possible candidates, creating a very large search space that makes the approach infeasible.

**Lemma 1.** *Let  $m$  be the number of distinct events in  $D_{SEQ}$ , and  $h$  be the longest length of a temporal pattern. The total number of temporal patterns in HPG from level  $L_1$  to level  $L_h$  is  $O(m^h 3^{h^2})$ .*

2) *Two-steps filtering approach*: Given the huge set of candidates, it is prohibitively expensive to check their support and confidence. To tackle this problem, we propose a *filtering approach* to reduce unnecessary candidate checking. More

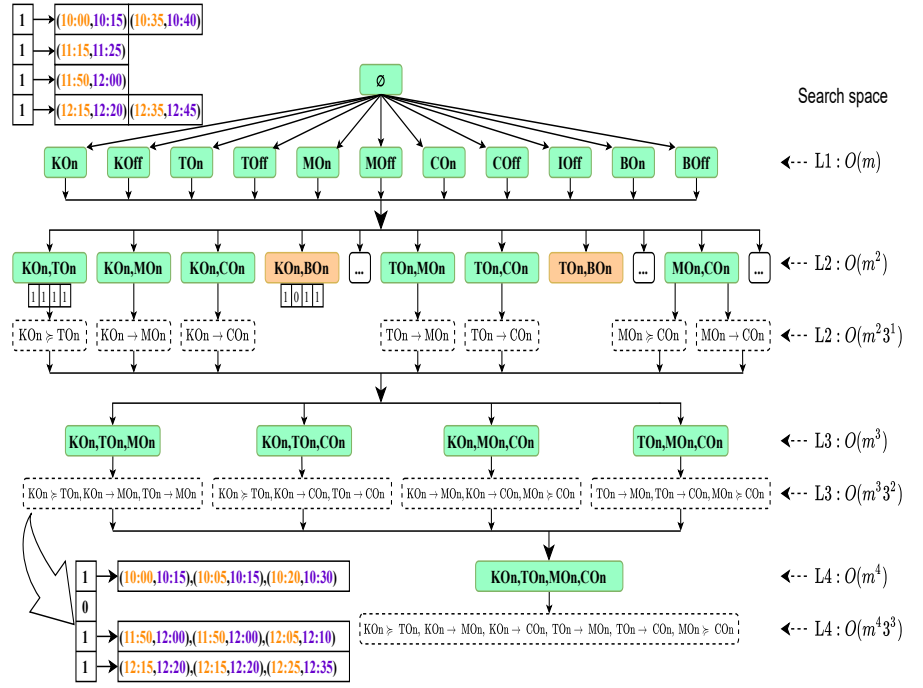


Fig. 4: A Hierarchical Pattern Graph for Table III

specifically, at any level  $h$  ( $h \geq 2$ ) in HPG, the mining process is divided into two steps: (1) first, it selects only frequent nodes (i.e., remove infrequent combinations of events), (2) second, it generates temporal patterns only from frequent nodes found in the first step. The correctness of this filtering approach is based on the following Apriori-inspired lemmas.

**Lemma 2.** *Let  $(E_i, E_j)$  be a pair of events occurs in a 2-event pattern  $P$ . Then,  $supp(P) \leq supp(E_i, E_j)$ .*

*Proof.* Derived directly from Defs. 3.11, 3.12, 3.13 and 3.14.  $\square$

Lemma 2 says that the support of a temporal pattern is always at most the support of the events occurring in it. Thus, if a pair of events does not satisfy the support threshold, it cannot occur in any frequent temporal patterns.

**Lemma 3.** *Let  $(E_i, E_j)$  be a pair of events occurs in a 2-event pattern  $P$ . Then  $conf(P) \leq conf(E_i, E_j)$ .*

*Proof.* Can derived directly from Defs. 3.15 and 3.16.  $\square$

From Lemma 3, the confidence of a temporal pattern  $P$  is always at most the confidence of the events present in it. Thus, if a pair of events does not satisfy the confidence threshold, it cannot occur in any high confident temporal patterns.

Applying Lemmas 2 and 3 to the first filtering step will remove infrequent or low confidence event pairs that cannot be present in frequent patterns. This helps reduce the pattern candidates while still ensuring the completeness of HTPGM. We detail the filtering approach below.

*Step 2.1. Mining frequent pairs of events*: This step selects only frequent event pairs in  $D_{SEQ}$ , using the set  $IFreq$  found in

$L_1$  of HPG. First, HTPGM generates all possible event pairs by calculating the Cartesian product  $IFreq \times IFreq$ . Next, for each event pair  $(E_i, E_j)$ , the *bitmap*  $b_{ij}$  is computed by *ANDing* the two individual bitmaps:  $b_{ij} = AND(b_i, b_j)$  ( $b_{ij}$  represents the set of sequences where both events occur). Finally, HTPGM computes the support  $supp(E_i, E_j)$  by counting the set bits in  $b_{ij}$ , and compares it against  $\sigma$ .

Assume that  $supp(E_i, E_j) \geq \sigma$ , thus  $(E_i, E_j)$  has high enough support. We continue filtering  $(E_i, E_j)$  by applying Lemma 3:  $(E_i, E_j)$  is selected only if its confidence is at least  $\delta$ . After this filtering, only frequent and high confident event pairs are selected. These pairs form the nodes in  $L_2$ .

*Step 2.2. Mining frequent patterns:* This step finds frequent 2-event patterns from the nodes in  $L_2$ . For each node  $(E_i, E_j) \in L_2$ , we use the *bitmap*  $b_{ij}$  to retrieve the set of sequences  $S$  where both events are present. Next, for each sequence  $S \in \mathcal{S}$ , the pairs of event instances  $(e_i, e_j)$  are extracted, and the relations between them are verified. The support and confidence of each relation  $r(E_{i \triangleright e_i}, E_{j \triangleright e_j})$  are computed and compared against the thresholds, after which only frequent relations are selected and stored in the corresponding node in  $L_2$ . Examples of the relations in  $L_2$  can be seen in Fig. 4. Note that the selected relations have similar data structures with the nodes they belong to, i.e., containing the relation *bitmap*, and the corresponding event instances.

This mining step results in two different sets of nodes in  $L_2$ . The first set contains nodes that are frequent but do not contain any frequent patterns. These nodes (colored in yellow in Fig. 4) are removed from  $L_2$ . The second set are nodes that contain frequent patterns (colored in green in Fig. 4). These nodes are kept in  $L_2$ , and will be used in the subsequent steps of the mining process.

*Complexity:* Let  $m$  be the number of frequent single events in  $L_1$ , and  $i$  be the average number of instances of each event. The complexity of frequent 2-event pattern mining is  $O(m^2 i^2 |D_{SEQ}|^2)$ .

## F. Mining Frequent $k$ -event Patterns

Mining frequent  $k$ -event patterns ( $k \geq 3$ ) follows a similar filtering process as 2-event patterns. However, with  $k \geq 3$ , we introduce additional pruning based on the transitivity property of temporal patterns.

*Step 1. Mining frequent  $k$ -event combinations:* This step finds frequent  $k$ -event combinations in  $L_k$  of HPG.

Let  $(k-1)Freq$  be the set of frequent  $(k-1)$ -event combinations found in  $L_{k-1}$ , and  $IFreq$  be the set of frequent single events in  $L_1$ . To generate all  $k$ -event combinations, the usual process is to compute the Cartesian product:  $(k-1)Freq \times IFreq$ . However, we observe that using  $IFreq$  to generate event combinations at level  $L_k$  can create redundancy, as  $IFreq$  might contain events that when combining with nodes in  $L_{k-1}$ , result in combinations that clearly cannot have any frequent patterns. To illustrate this observation, consider node BOn at  $L_1$  in Fig. 4. Here, BOn is a frequent event, and thus, can be combined with frequent nodes in  $L_2$  such as (KOn, TOn) to create a 3-event combination (KOn, TOn, BOn). However,

(KOn, TOn, BOn) cannot form any frequent 3-event patterns, since BOn does not create any frequent 2-event patterns in  $L_2$ . To reduce the redundancy, the combination (KOn, TOn, BOn) should not be created in the first place. We rely on the *transitivity property* of temporal relations to identify such event combinations.

**Lemma 4.** *Let  $S = \langle e_1, \dots, e_{n-1} \rangle$  be a temporal sequence that supports an  $(n-1)$ -event pattern  $P = \langle (E_{1 \triangleright e_1}, r_{12}, E_{2 \triangleright e_2}), \dots, (E_{n-2 \triangleright e_{n-2}}, r_{(n-2)(n-1)}, E_{n-1 \triangleright e_{n-1}}) \rangle$ .*

*Let  $e_n$  be an event instance that is combined with  $S$  to create a new temporal sequence  $S' = \langle e_1, \dots, e_n \rangle$ . Then the set of temporal relations  $\mathfrak{R}$  is transitive on  $S'$ :  $\forall e_i \in S', i \neq n, \exists r \in \mathfrak{R}$  s.t.  $r(E_{i \triangleright e_i}, E_{n \triangleright e_n})$  holds.*

Lemma 4 says that, a new event instance can always form temporal relations with existing instances of an existing temporal sequence. Based on this transitivity property, we can prove the following lemma.

**Lemma 5.** *Let  $N_{k-1} = (E_1, \dots, E_{k-1})$  be a frequent combination of  $(k-1)$  events, and  $E_k$  be a frequent single event. The combination  $N_k = N_{k-1} \cup E_k$  cannot form any frequent  $k$ -event temporal patterns if  $\nexists E_i \in N_{k-1}, r \in \mathfrak{R}$  s.t.  $r(E_i, E_k)$  is a frequent temporal relation.*

From Lemma 5, only single events in  $L_1$  that form at least one frequent pattern in  $L_{k-1}$  should be used to create event combinations in  $L_k$ . Based on this result, we perform an initial filtering on  $IFreq$  ahead of the Cartesian product calculation. Specifically, from the nodes in level  $L_{k-1}$ , we extract the distinct single events  $D_{k-1}$ , and *intersect* them with  $IFreq$  to remove redundant single events:  $FilteredIFreq = D_{k-1} \cap IFreq$ . Then, the Cartesian product  $(k-1)Freq \times FilteredIFreq$  is calculated to generate all possible  $k$ -event combinations. Next, we apply Lemmas 2 and 3 to select only frequent and high confident  $k$ -event combinations  $kFreq$  to form  $L_k$ .

*Step 2. Mining frequent  $k$ -event patterns:* This step finds frequent  $k$ -event patterns from the nodes in  $L_k$ . Unlike 2-event patterns, determining the relations in a  $k$ -event combination ( $k \geq 3$ ) is much more expensive, as it requires to verify the frequency of  $\frac{1}{2}k(k-1)$  triples. To reduce the cost of relation checking, we propose an iterative verification approach that also relies on the *transitivity property* of temporal relations.

**Lemma 6.** *Consider two temporal patterns  $P$  and  $P'$ . If  $P' \subseteq P$ , then  $conf(P') \geq conf(P)$ .*

**Lemma 7.** *Consider two temporal patterns  $P$  and  $P'$ . If  $P' \subseteq P$  and  $\frac{supp(P')}{\max_{1 \leq k \leq |P'|} \{supp(E_k)\}_{E_k \in P'}} \leq \delta$ , then  $conf(P) \leq \delta$ .*

Lemmas 6, 7 say that a temporal pattern  $P$  cannot be high confident if any of its sub-patterns does not satisfy the confidence threshold.

Let  $N_{k-1} = (E_1, \dots, E_{k-1})$  be a node in  $L_{k-1}$ ,  $N_1 = (E_k)$  be a node in  $L_1$ , and  $N_k = N_{k-1} \cup N_1 = (E_1, \dots, E_k)$  be a node in  $L_k$ . To find  $k$ -event patterns for  $N_k$ , we first retrieve the set  $P_{k-1}$  containing frequent  $(k-1)$ -event patterns in node  $N_{k-1}$ . Assume that

$s = \langle e_1, \dots, e_{k-1} \rangle$  is the sequence that supports the pattern  $p_{k-1}$ . Then,  $p_{k-1}$  is a list of  $\frac{1}{2}(k-1)(k-2)$  triples:  $p_{k-1} \{ (E_{1 \triangleright e_1}, r_{12}, E_{2 \triangleright e_2}), \dots, (E_{k-2 \triangleright e_{k-2}}, r_{(k-2)(k-1)}, E_{k-1 \triangleright e_{k-1}}) \}$ . In order for  $p_{k-1}$  to be frequent and high confident in node  $N_{k-1}$ , each of the triples  $(E_{i \triangleright e_i}, r_{ij}, E_{j \triangleright e_j}) \in p_{k-1}$  must be frequent (Lemmas 4 and 5) and high confident (Lemmas 4, 6, and 7). For each  $p_{k-1}$ , we iteratively verify the possibility of  $p_{k-1}$  forming a frequent k-event pattern with  $E_k$  as follows.

We first check whether the triple  $(E_{k-1 \triangleright e_{k-1}}, r_{(k-1)k}, E_{k \triangleright e_k})$  is frequent and high confident by accessing the node  $(E_{k-1}, E_k)$  in  $L_2$ . If the triple is not frequent or high confident, the verifying process stops immediately for  $p_{k-1}$ . Otherwise, it continues on the triple  $(E_{k-2 \triangleright e_{k-2}}, r_{(k-2)k}, E_{k \triangleright e_k})$ , until it reaches  $(E_{1 \triangleright e_1}, r_{1k}, E_{k \triangleright e_k})$ .

**Complexity:** Let  $r$  be the average number of frequent (k-1)-event patterns in each node of  $L_{k-1}$ . The complexity of frequent k-event pattern mining is  $O(|IFreq| \cdot |L_{k-1}| \cdot r \cdot k^2 \cdot |\mathcal{D}_{SEQ}|)$ .

Algorithm 1 provides the pseudo code of HTPGM, consisting of 3 mining steps.

---

**Algorithm 1:** Hierarchical Temporal Pattern Graph Mining (HTPGM)

---

**Input:** A set of time series  $\mathcal{X}$ , a minimum support threshold  $\sigma$ , a minimum confidence threshold  $\delta$

**Output:** The set of frequent temporal patterns  $P$

- 1: **Function** Frequent Single Event ( $\mathcal{D}_{SEQ}$ )
- 2:   **foreach** event  $E_i \in \mathcal{D}_{SEQ}$  **do**
- 3:      $supp(E_i) \leftarrow \text{countBitmap}(b_i)$ ;
- 4:     **if**  $supp(E_i) \geq \sigma$  **then**
- 5:        $IFreq \leftarrow E_i$ ;
- 6:     **return**  $IFreq$ ;
- 7: **Function** Frequent 2-event Patterns ( $\mathcal{D}_{SEQ}$ ,  $IFreq$ )
- 8:   EventPairs  $\leftarrow$  Cartesian( $IFreq, IFreq$ );
- 9:   FrequentEventPairs  $\leftarrow$  Apriori\_Filtering(EventPairs);
- 10: **foreach** pair in FrequentEventPairs **do**
- 11:    Retrieve relations;
- 12:    Check frequent relations;
- 13: **return**  $2Freq$ ;
- 14: **Function** Frequent k-event Patterns ( $\mathcal{D}_{SEQ}$ ,  $(k-1)Freq, IFreq$ )
- 15:   Filtered1Freq  $\leftarrow$  Transitivity\_Filtering( $IFreq$ );
- 16:   EventCombinations  $\leftarrow$  Cartesian(Filtered1Freq,  $(k-1)Freq$ );
- 17:   FrequentEventCombinations  $\leftarrow$  Apriori\_Filtering(EventCombinations);
- 18: **foreach** combination in FrequentEventCombinations **do**
- 19:    Retrieve relations;
- 20:    Iteratively check frequent relations;
- 20: **return**  $kFreq$ ;

---

## V. APPROXIMATE MINING USING MUTUAL INFORMATION

In this section, we first use mutual information (MI) to derive the lower bound of confidence for an event pair, and show that frequent temporal patterns extracted from *correlated* symbolic time series have confidences above this bound. Based on this result, we propose an approximation for HTPGM that mines frequent temporal patterns only from the  $\mathcal{D}_{SYB}$  subset of

*correlated* symbolic time series, and thus, significantly reduces the search space. Our experiments in Section VI also show that temporal patterns extracted from *uncorrelated* time series are typically infrequent with low confidence, and thus, are generally not interesting to explore. Below, we review the concepts of entropy and mutual information, and then use them to define *correlated* symbolic time series. Next, we derive the confidence lower bound of an event pair, and discuss how to use the derived bound to approximate HTPGM.

### A. Correlated symbolic time series

**Definition 5.1** (Entropy) The *entropy* of a symbolic time series  $\mathcal{X}_S$ , denoted as  $H(\mathcal{X}_S)$ , is defined as

$$H(\mathcal{X}_S) = - \sum_{x \in \Sigma_X} p(x) \cdot \log p(x) \quad (7)$$

where  $\Sigma_X$  is the symbolic alphabet of  $\mathcal{X}_S$ . Intuitively, the entropy measures the amount of information or uncertainty inherent in the possible outcomes of a random variable. The higher the  $H(\mathcal{X}_S)$ , the more uncertain the outcome of  $\mathcal{X}_S$ .

The conditional entropy  $H(\mathcal{X}_S | \mathcal{Y}_S)$  quantifies the amount of information needed to describe the outcome of  $\mathcal{X}_S$ , given the value of  $\mathcal{Y}_S$ , and is defined as

$$H(\mathcal{X}_S | \mathcal{Y}_S) = - \sum_{x \in \Sigma_X} \sum_{y \in \Sigma_Y} p(x, y) \cdot \log \frac{p(x, y)}{p(y)} \quad (8)$$

**Definition 5.2** (Mutual information) The *mutual information* of two symbolic time series  $\mathcal{X}_S$  and  $\mathcal{Y}_S$ , denoted as  $I(\mathcal{X}_S; \mathcal{Y}_S)$ , is defined as

$$I(\mathcal{X}_S; \mathcal{Y}_S) = \sum_{x \in \Sigma_X} \sum_{y \in \Sigma_Y} p(x, y) \cdot \log \frac{p(x, y)}{p(x) \cdot p(y)} \quad (9)$$

where  $\Sigma_X$  and  $\Sigma_Y$  are the symbol alphabets of  $\mathcal{X}_S$  and  $\mathcal{Y}_S$ , respectively. The mutual information represents the reduction of uncertainty of one variable (e.g.,  $\mathcal{X}_S$ ), given the knowledge of another variable (e.g.,  $\mathcal{Y}_S$ ). The larger  $I(\mathcal{X}_S; \mathcal{Y}_S)$ , the more information is shared between  $\mathcal{X}_S$  and  $\mathcal{Y}_S$ , and thus, the less uncertainty about one variable when knowing the other.

We demonstrate how to compute the MI between the symbolic series  $K$  and  $T$  in Table I. We have:  $p(\text{KOn}) = \frac{17}{36}$ ,  $p(\text{KOff}) = \frac{19}{36}$ ,  $p(\text{TOn}) = \frac{18}{36}$ , and  $p(\text{TOff}) = \frac{18}{36}$ . We also have:  $p(\text{KOn, TOn}) = \frac{15}{36}$ ,  $p(\text{KOff, TOff}) = \frac{15}{36}$ ,  $p(\text{KOn, TOff}) = \frac{2}{36}$ , and  $p(\text{KOff, TOn}) = \frac{4}{36}$ . Using Eq. 9, we have  $I(K; T) = 0.29$ .

The MI is equal to zero if and only if the considered variables are statistically independent, and always positive if they have any kind of dependency (e.g. linear, non-linear). This property makes MI a versatile measure to capture correlations between variables. However, since  $0 \leq I(\mathcal{X}_S; \mathcal{Y}_S) \leq \min(H(\mathcal{X}_S), H(\mathcal{Y}_S))$  [9], the upper bound of MI values is unbounded. To scale the MI value into the range  $[0 - 1]$ , we use normalized mutual information as defined below.

**Definition 5.3** (Normalized mutual information) The *normalized mutual information* (NMI) of two random variables  $X$  and  $Y$ , denoted as  $\tilde{I}(\mathcal{X}_S; \mathcal{Y}_S)$ , is defined as

$$\tilde{I}(\mathcal{X}_S; \mathcal{Y}_S) = \frac{I(\mathcal{X}_S; \mathcal{Y}_S)}{H(\mathcal{X}_S)} = 1 - \frac{H(\mathcal{X}_S | \mathcal{Y}_S)}{H(\mathcal{X}_S)} \quad (10)$$

By dividing the MI with the entropy,  $\tilde{I}(\mathcal{X}_S; \mathcal{Y}_S)$  represents the percentage of reduction of uncertainty about  $\mathcal{X}_S$  due to knowing  $\mathcal{Y}_S$ . Based on Eq. 10, any pair of variables  $(\mathcal{X}_S, \mathcal{Y}_S)$  that has  $\tilde{I}(\mathcal{X}_S; \mathcal{Y}_S) > 0$  will hold a certain degree of mutual dependency. Moreover, Eq. 10 also shows that NMI is not symmetric, i.e.,  $\tilde{I}(\mathcal{X}_S; \mathcal{Y}_S) \neq \tilde{I}(\mathcal{Y}_S; \mathcal{X}_S)$ .

Using Table I, we have  $I(K; T) = 0.29$ . However, we do not know what the 0.29 reduction means in practice. Using NMI in Eq. 10, we have  $\tilde{I}(K; T) = 0.43$ , which says that the uncertainty of  $K$  is reduced by 43% given  $T$ . Moreover, we have  $\tilde{I}(T; K) = 0.42$ , showing that  $\tilde{I}(K; T) \neq \tilde{I}(T; K)$ .

**Definition 5.4** (Correlated symbolic time series) Let  $\mu$  ( $0 < \mu \leq 1$ ) be the mutual information threshold, and  $\mathcal{X}_S$  and  $\mathcal{Y}_S$  be the symbolic representations of the time series  $X$  and  $Y$ , respectively. We say that the symbolic time series  $\mathcal{X}_S$  and  $\mathcal{Y}_S$  are *correlated* iff  $\tilde{I}(\mathcal{X}_S; \mathcal{Y}_S) \geq \mu$ , and *uncorrelated* otherwise.

### B. Lower Bound of the Confidence

Consider two time series  $X$  and  $Y$ , and their corresponding symbolic series  $\mathcal{X}_S$  and  $\mathcal{Y}_S$ . Let  $X_1$  be a temporal event of  $X$ ,  $Y_1$  be a temporal event of  $Y$ , and  $\mathcal{D}_{\text{SYB}}$ ,  $\mathcal{D}_{\text{SEQ}}$  be the symbolic database and the temporal sequence database created from  $\mathcal{X}_S$  and  $\mathcal{Y}_S$ , respectively. We first study the relationship between the supports of  $(X_1, Y_1)$  in  $\mathcal{D}_{\text{SYB}}$  and  $\mathcal{D}_{\text{SEQ}}$ .

**Lemma 8.** Let  $\text{supp}(X_1, Y_1)_{\mathcal{D}_{\text{SYB}}}$  be the support of  $(X_1, Y_1)$  in  $\mathcal{D}_{\text{SYB}}$ , and  $\text{supp}(X_1, Y_1)_{\mathcal{D}_{\text{SEQ}}}$  be the support of  $(X_1, Y_1)$  in  $\mathcal{D}_{\text{SEQ}}$ . We have:  $\text{supp}(X_1, Y_1)_{\mathcal{D}_{\text{SYB}}} \leq \text{supp}(X_1, Y_1)_{\mathcal{D}_{\text{SEQ}}}$ .

Lemma 8 says that, if an event pair is frequent in  $\mathcal{D}_{\text{SYB}}$ , it is also frequent in  $\mathcal{D}_{\text{SEQ}}$ . We now investigate the connection between the NMI of  $\mathcal{X}_S$  and  $\mathcal{Y}_S$  in  $\mathcal{D}_{\text{SYB}}$ , i.e.,  $\tilde{I}(\mathcal{X}_S; \mathcal{Y}_S)$ , and the confidence of the event pair  $(X_1, Y_1)$  in  $\mathcal{D}_{\text{SEQ}}$  below.

**Theorem 1.** Let  $\sigma$  be the minimum support threshold, and  $\mu$  be the mutual information threshold. Let  $\sigma_m$  be the maximum support an event pair  $(X_1, Y_1)$  can have. Assume that  $(X_1, Y_1)$  is frequent in  $\mathcal{D}_{\text{SYB}}$ , i.e.,  $\sigma \leq \text{supp}(X_1, Y_1)_{\mathcal{D}_{\text{SYB}}} \leq \sigma_m$ .

If  $\tilde{I}(\mathcal{X}_S; \mathcal{Y}_S) \geq \mu$ , then  $\text{conf}(X_1, Y_1)_{\mathcal{D}_{\text{SEQ}}}$  has a lower bound LB:  $\text{conf}(X_1, Y_1)_{\mathcal{D}_{\text{SEQ}}} \geq \text{LB}$  where

$$\text{LB} = \left( \sigma^{\sigma_m} \cdot \left( \frac{1 - \sigma_m}{n_x - 1} \right)^{1 - \sigma} \right)^{\frac{1 - \mu}{\sigma}} \cdot \frac{\sigma}{2 \cdot \sigma_m - \sigma} \quad (11)$$

where  $n_x$  is the number of symbols in the symbol alphabet  $\Sigma_X$ .

From Theorem 1, if  $X_S$  and  $Y_S$  are correlated w.r.t.  $\mu$ , then a frequent event pair formed by  $(X_S, Y_S)$  has a confidence of at least the given bound LB (Eq. (11)) in  $\mathcal{D}_{\text{SEQ}}$ . Combining Theorem 1 and Lemma 3, we can say that if an event pair has a confidence less than the lower bound LB, then any temporal pattern  $P$  containing that event pair also has the confidence less than LB. Based on this result, we propose an approximation for HTPGM, described in the next section.

### C. Approximate HTPGM using the Confidence Lower Bound

Using the confidence lower bound in Theorem 1, HTPGM can be approximated by first finding a set of correlated

symbolic time series  $\mathcal{X}_C \subseteq \mathcal{X}$ , and then performing the mining only on  $\mathcal{X}_C$ . To explain how HTPGM can mine using  $\mathcal{X}_C$ , we first define a correlation graph.

**Definition 5.5** (Correlation graph) A *correlation graph* is an *undirected* graph  $G_C = (V, E)$  where  $V$  is the set of vertices, and  $E$  is the set of edges. Each vertex  $v_i \in V$  represents one symbolic series  $\mathcal{X}_i \in \mathcal{X}_C$ . There is an edge  $e_{ij}$  between a vertex  $v_i$  containing  $\mathcal{X}_i$ , and a vertex  $v_j$  containing  $\mathcal{X}_j$  iff  $\tilde{I}(\mathcal{X}_i; \mathcal{X}_j) \geq \mu \wedge \tilde{I}(\mathcal{X}_j; \mathcal{X}_i) \geq \mu$ .

Since NMI is not symmetric, in a correlation graph, there is an edge between two vertices only if their NMIs satisfy  $\mu$  in both directions. Thus, the correlation graph is undirected. Moreover, to set the value of  $\mu$ , we propose to rely on the density of the correlation graph.

**Definition 5.6** (Correlation graph density) Given a correlation graph  $G_C$ , the *correlation graph density*  $d_{G_C}$  is measured as the ratio between the number of edges in  $G_C$  and the number of edges in the corresponding complete graph.

The value of  $d_{G_C}$  represents the number of edges remains  $G_C$  (or infers the number of edges pruned from the complete graph). The higher  $\mu$ , the more edges remain in  $G_C$ , and thus, few edges are pruned. Using the correlation graph density, we can choose  $\mu$  such that it satisfies a given expected density  $\mathbb{E}(d_{G_C})$ . As an example, consider  $\mathcal{D}_{\text{SYB}}$  in Table I which has 6 symbolic series. The complete graph of 6 vertices (each corresponds to one symbolic series) has 15 edges. If we set the density of the correlation graph to be 40%, then  $G_C$  will have:  $15 \times 40\% \approx 6$  edges, which corresponds to  $\mu = 0.42$ . Fig. 5 shows an example of  $G_C$  built from  $\mathcal{D}_{\text{SYB}}$  in Table I.

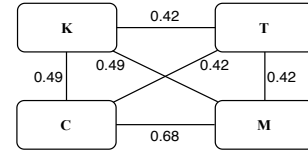


Fig. 5: Correlation graph

Algorithm 2 illustrates how HTPGM can be approximated using the correlation graph  $G_C$ . First, to find the set  $\mathcal{X}_C$ , we compute NMI for each pair of symbolic series  $(\mathcal{X}_S, \mathcal{Y}_S)$  in  $\mathcal{D}_{\text{SYB}}$  (line 3). Next, only the pair that has both  $\tilde{I}(\mathcal{X}_S; \mathcal{Y}_S)$  and  $\tilde{I}(\mathcal{Y}_S; \mathcal{X}_S)$  at least  $\mu$  are selected and inserted into  $\mathcal{X}_C$  (lines 4-5), and create an edge between  $\mathcal{X}_S$  and  $\mathcal{Y}_S$  in the correlation graph (line 6). Next, at level  $L_1$  of HPG, only the correlated symbolic series present in  $\mathcal{X}_C$  are used to generate single events (lines 7-8). At  $L_2$ , the correlation graph is used to filter 2-event combinations, adding an additional filtering step to HTPGM as follows.

For each event pair  $(E_i, E_j)$ , we check whether there is an edge between the symbolic series of  $E_i$  and of  $E_j$  in  $G_C$ . If so, we proceed on computing the support and confidence of  $(E_i, E_j)$  as in the exact HTPGM (lines 9-11). Otherwise,  $(E_i, E_j)$  is eliminated from the mining of  $L_2$ . From level  $L_k$  ( $k \geq 3$ ) onwards, the mining is the same as for the exact HTPGM (lines 12-13).

---

**Algorithm 2:** Approximate HTPGM using MI

---

**Input:** A set of time series  $\mathcal{X}$ , a minimum MI threshold  $\mu$ , minimum support threshold  $\sigma$ , maximum support threshold  $\sigma_m$ , minimum confidence threshold  $\delta$   
**Output:** The set of frequent temporal patterns  $P$

- 1: convert  $\mathcal{X}$  to  $\mathcal{D}_{\text{SYB}}$  and  $\mathcal{D}_{\text{SEQ}}$ ;
- 2: **foreach** pair of symbolic time series  $(\mathcal{X}_S, \mathcal{Y}_S) \in \mathcal{D}_{\text{SYB}}$  **do**
- 3:   compute  $\tilde{I}(\mathcal{X}_S; \mathcal{Y}_S)$  and  $\tilde{I}(\mathcal{Y}_S; \mathcal{X}_S)$ ;
- 4:   **if**  $\tilde{I}(\mathcal{X}_S; \mathcal{Y}_S) \geq \mu \wedge \tilde{I}(\mathcal{Y}_S; \mathcal{X}_S) \geq \mu$  **then**
- 5:     insert  $\mathcal{X}_S$  and  $\mathcal{Y}_S$  into  $\mathcal{X}_C$ ;
- 6:     create an edge between  $\mathcal{X}_S$  and  $\mathcal{Y}_S$  in  $G_C$ ;
- 7: **foreach**  $\mathcal{X}_i \in \mathcal{X}_C$  **do**
- 8:   Mine frequent single events from  $\mathcal{X}_i$ ;
- 9: **foreach** event pair  $(E_i, E_j)$  **do**
- 10:   **if** There is an edge between  $\mathcal{X}_i$  and  $\mathcal{X}_j$  in  $G_C$  **then**
- 11:     Mine frequent patterns for  $(E_i, E_j)$ ;
- 12: **if**  $k \geq 3$  **then**
- 13:   Perform HTPGM using  $L_1$  and  $L_2$ ;

---

TABLE IV: Characteristics of the datasets

	NIST [12]	UKDALE [16]	DataPort [11]	Smart City [8]
# of sequences	1460	1520	1210	1216
# of variables	72	53	21	59
# of distinct events	144	106	42	118
Avg. # of instances/sequence	140	126	163	155

*Complexity analysis:* To compute the NMI, we first scan  $\mathcal{D}_{\text{SYB}}$  once to compute the probability of each individual event. Thus, the complexity of NMI computation is  $|\mathcal{D}_{\text{SYB}}|$ .

On the other hand, the complexity to mine frequent 2-event patterns in HTPGM is  $O(m^2 i^2 |\mathcal{D}_{\text{SEQ}}|^2)$ . Thus, we can expect that using approximate HTPGM with mutual information can significantly improve the performance of HTPGM.

## VI. EXPERIMENTAL EVALUATION

We evaluate HTPGM (both exact and approximate), using real-world datasets from two application domains: smart energy and smart city. The evaluation is both qualitative (to assess the quality of extracted patterns) and quantitative (to evaluate the scalability and efficiency of HTPGM).

### A. Experimental Setup

1) *Datasets:* We use 3 *smart energy datasets*: NIST [12], UKDALE [16], and DataPort [11], all of which measure the energy/power consumption of electrical appliances in residential households. For the *smart city datasets*, we use weather and vehicle collision datasets obtained from NYC Open Data Portal [8]. The datasets contain information about weather conditions, and the collision incidents in New York City. Table IV summarizes the characteristics of each dataset when converting to  $\mathcal{D}_{\text{SEQ}}$ .

2) *Obtaining symbolic representations:* Data collected from the energy and smart city datasets are numerical time series which need to be converted into symbolic representations. For the energy datasets, the symbol alphabet  $\Sigma$  contains only two symbols: On and Off. The threshold for an On symbol is  $v_t \geq 0.05$ , and Off otherwise ( $v_t$  is the time series value at time  $t$ ).

Unlike the energy data, weather conditions and vehicle collisions have more than 2 states. For example, temperature

can be classified into {Very Cold, Cold, Mild, Hot, Very Hot}, or the number of injuries can be categorized as {None, Low, Medium, High}. To define the mapping function between  $\Sigma$  and the time series values, we rely on the percentile distribution of data. The percentile values depend on the specific variables. For example, we use 10th, 25th, 50th, 75th, 95th percentiles for a variable that has 5 states.

3) *Baseline methods:* Our exact method is referred to as E-HTPGM, and the approximate one as A-HTPGM. We use 3 different baselines (description in Section II): (1) TPMiner [7], (2) IEMiner [21], and (3) H-DFS [20]. These methods are the most well-known in TPM. Moreover, since both E-HTPGM and the baselines provide the same exact solutions, we only use the baselines for quantitative evaluation, and compare qualitatively only between E-HTPGM and A-HTPGM.

4) *Infrastructure:* All methods, E-HTPGM, A-HTPGM and the baselines are implemented in Python. The experiments are run on a single machine with Intel Core i7-4770HQ (2.2GHz) CPU, 16 GB main memory.

### B. Qualitative Evaluation

In this evaluation, our goal is to make sense and learn insights from extracted patterns. Due to space limitations, we discuss just a few of them below.

1) *Generated temporal patterns:* We first summarize in Table V the number of extracted patterns for each dataset. We can see that, the Smart City dataset generate more patterns than the energy datasets, since its variables have more states than the energy ones.

2) *Interpretation of extracted patterns:* Table VI summarizes some interesting patterns we found in the datasets, together with the support and confidence. Patterns P1 - P11 are extracted from the energy datasets, which show that through analyzing the interactions of the residents with electrical devices, we can understand their living patterns/habits. Patterns P12 - P17 show the association between weather conditions and the collision situations. Such patterns indicate that extreme or abnormal weather conditions are linked to a high number of collisions. Moreover, they occur with low support but high confidence, implying that such patterns are rare, but with strong confidence of the association.

### C. Quantitative Evaluation

1) *Baselines comparison:* We compare E-HTPGM and A-HTPGM with the baselines in terms of the runtimes and the memory usage. In this experiment, A-HTPGM is run with 4 different values of  $\mu$  (80%, 60%, 40%, 20%) which correspond to 80%, 60%, 40%, and 20% of the edges in the correlation graph. Tables VII and VIII show the results on the NIST and Smart City datasets (we do not show other datasets due to the space limitations, but they give similar results).

It can be seen that E-HTPGM and A-HTPGM have better performance (both the runtimes and the memory usage) than the baselines, with A-HTPGM achieves the best performance among all methods. On tested datasets, the range and average speedups of E-HTPGM compared to the baselines are: [1.3 –

TABLE V: Summary of Extracted Patterns

Support (%)	Confidence (%)															
	NIST				UKDALE				DataPort				Smart City			
	20	40	60	80	20	40	60	80	20	40	60	80	20	40	60	80
20	519,316	378,896	69,951	28,912	126,490	39,629	10,562	4,231	310,713	200,179	11,074	5,012	1,201,723	1,001,354	121,140	7,164
40	96,952	96,952	46,793	14,193	46,193	26,172	8,240	4,129	201,561	140,984	8,928	4,813	91,241	90,198	76,014	6,891
60	29,955	29,955	29,955	9,608	11,247	6,221	5,392	3,921	9,781	7,229	6,582	3,827	13,126	8,712	6,286	6,140
80	3,568	3,568	3,568	3,568	4,832	4,321	3,251	3,251	5,492	4,825	3,981	3,370	7,018	6,872	6,002	6,002

TABLE VI: Summary of Interesting Patterns

Patterns	Supp. %	Conf. %
(P1) ([05:58, 08:24] First Floor Lights On) $\succ$ ([05:58, 06:59] Upstairs Bathroom Lights On) $\succ$ ([05:59, 06:06] Microwave On)	20	30
(P2) ([06:00, 07:01] Upstairs Bathroom Lights On) $\succ$ ([06:40, 06:46] Upstairs Bathroom Plugs On)	30	20
(P3) ([18:00, 18:30] Lights Dining Room On) $\rightarrow$ ([18:31, 20:16] Children Room Plugs On) $\hat{=}$ ([19:00, 22:31] Lights Living Room On)	20	20
(P4) ([15:59, 16:05] Hallway Lights On) $\rightarrow$ ([17:58, 18:29] Kitchen Lights On $\succ$ ([18:00, 18:18] Plug In Kitchen On) $\succ$ ([18:08, 18:15] Microwave On)	80	60
(P5) ([06:02, 06:19] Kitchen Lights On) $\rightarrow$ ([06:05, 06:12] Microwave On) $\hat{=}$ ([06:09, 06:11] Kettle On)	20	5
(P6) ([05:58,08:24] First Floor Lights On) $\succ$ ([05:58,06:59] Upstairs Bathroom Lights On) $\succ$ ([05:59, 06:06] Microwave On)	20	30
(P7) ([06:00,07:01] Upstairs Bathroom Lights On) $\succ$ ([06:40,06:46] Upstairs Bathroom Plugs On)	30	20
(P8) ([18:10,18:15] Kitchen App) $\rightarrow$ ([18:15,19:00] Lights Plugs) $\succ$ ([18:20,18:25] Microwave) $\rightarrow$ ([18:25,18:55] Cooktop) $\rightarrow$ ([19:30,20:20] Clothes Dryer)	5	50
(P9) ([16:45, 17:30] Clothes Washer) $\rightarrow$ ([17:40,18:55] Clothes Dryer) $\rightarrow$ ([19:05, 20:10] Dining Room) $\succ$ ([19:10, 19:30] Cooktop)	10	30
(P10) ([06:10, 07:00] Kitchen Lights) $\succ$ ([06:10, 06:15] Kettle) $\rightarrow$ ([06:30, 06:40] Toaster) $\rightarrow$ ([06:45, 06:48] Microwave)	25	40
(P11) ([18:00, 18:25] Kitchen Lights) $\succ$ ([18:00, 18:05] Kettle) $\rightarrow$ ([18:05, 18:10] Microwave) $\rightarrow$ ([19:35, 20:50] Washing Machine)	20	40
(P12) ([13:10, 22:35] Heavy Rain) $\succ$ ([14:00, 22:35] Unclear Visibility) $\succ$ ([15:00, 20:55] Overcast Cloudiness) $\rightarrow$ ([21:00, 21:55] High Motorist Collision)	5	30
(P13) ([19:00, 21:50] Unclear Extremely Visibility) $\succ$ ([19:00, 21:50] High Snow) $\succ$ ([20:00, 20:55] High Motorist Collision)	30	45
(P14) Very Strong Wind $\rightarrow$ High Motorist Injury	5	40
(P15) Frost Temperature $\rightarrow$ Medium Cyclist Injury	5	20
(P16) Strong Wind $\rightarrow$ High Pedestrian Killed	4	30
(P17) Strong Wind $\rightarrow$ High Motorist Killed	4	10

TABLE VII: Runtime Comparison (seconds)

Support (%)	Methods	Confidence (%)					
		NIST			Smart City		
		20	50	80	20	50	80
20	H-DFS	23391.83	319.17	87.11	2516.64	223.47	10.27
	IEMiner	21615.74	219.59	77.24	1419.51	130.80	8.59
	TPMiner	3919.40	214.96	67.30	418.25	118.89	6.66
	E-HTPGM	410.81	50.92	16.59	136.53	46.42	3.38
	A-HTPGM (80%)	173.43	35.85	15.81	78.69	29.02	3.05
	A-HTPGM (60%)	21.23	20.48	15.43	24.61	10.67	2.42
	A-HTPGM (40%)	20.74	19.98	14.43	21.70	9.54	2.19
	A-HTPGM (20%)	<b>19.25</b>	<b>18.68</b>	<b>13.15</b>	<b>15.61</b>	<b>8.71</b>	<b>2.05</b>
50	H-DFS	830.17	190.06	83.62	453.47	88.32	9.82
	IEMiner	419.59	171.30	72.37	300.8	73.81	7.81
	TPMiner	214.96	144.05	62.78	118.89	37.54	6.14
	E-HTPGM	49.92	31.49	14.66	86.42	16.75	3.12
	A-HTPGM (80%)	22.12	21.09	13.52	12.34	12.30	2.84
	A-HTPGM (60%)	18.03	15.03	13.00	11.71	6.15	2.29
	A-HTPGM (40%)	17.83	14.07	12.65	6.34	6.11	2.19
	A-HTPGM (20%)	<b>16.68</b>	<b>12.73</b>	<b>12.58</b>	<b>6.20</b>	<b>5.86</b>	<b>2.03</b>
80	H-DFS	157.11	68.39	59.35	13.27	8.39	4.41
	IEMiner	107.24	63.42	58.39	9.59	5.47	4.37
	TPMiner	57.30	55.02	50.73	6.66	3.44	3.37
	E-HTPGM	17.59	14.60	12.66	3.38	1.96	1.67
	A-HTPGM (80%)	16.74	13.78	11.88	2.50	1.52	1.49
	A-HTPGM (60%)	16.60	13.66	11.72	2.45	1.18	1.09
	A-HTPGM (40%)	14.66	12.63	11.19	2.15	1.15	1.06
	A-HTPGM (20%)	<b>13.15</b>	<b>11.62</b>	<b>10.34</b>	<b>1.32</b>	<b>1.13</b>	<b>1.05</b>

TABLE VIII: Memory Usage Comparison (MB)

Support (%)	Methods	Confidence (%)					
		NIST			Smart City		
		20	50	80	20	50	80
20	H-DFS	3353.3	1519.13	796.45	1293.28	412.14	57.89
	IEMiner	2942.37	1015.79	675.51	1197.74	353.18	55.92
	TPMiner	2487.52	895.61	424.36	1002.82	254.26	51.23
	E-HTPGM	1870.45	356.58	185.41	807.41	167.85	46.13
	A-HTPGM (80%)	1250.22	316.67	174.09	594.90	145.39	43.36
	A-HTPGM (60%)	326.39	214.61	164.32	297.68	129.82	42.61
	A-HTPGM (40%)	248.52	208.40	161.69	265.84	129.24	41.89
	A-HTPGM (20%)	<b>222.39</b>	<b>204.61</b>	<b>158.93</b>	<b>257.68</b>	<b>128.82</b>	<b>40.76</b>
50	H-DFS	2070.57	971.66	627.00	1040.56	470.49	92.81
	IEMiner	1867.60	890.14	591.58	870.64	460.52	60.87
	TPMiner	1078.42	671.18	502.83	660.66	150.68	58.98
	E-HTPGM	328.41	269.21	162.25	144.13	134.07	46.04
	A-HTPGM (80%)	262.34	263.25	162.09	142.59	127.49	43.15
	A-HTPGM (60%)	192.82	169.89	160.69	130.76	122.88	42.83
	A-HTPGM (40%)	171.99	168.36	150.04	122.36	121.23	41.36
	A-HTPGM (20%)	<b>167.82</b>	<b>144.34</b>	<b>140.53</b>	<b>120.03</b>	<b>119.93</b>	<b>40.62</b>
80	H-DFS	794.19	589.09	549.88	249.78	139.59	63.65
	IEMiner	656.12	518.44	501.93	149.45	119.83	59.59
	TPMiner	486.57	482.34	476.74	119.59	69.91	59.63
	E-HTPGM	162.82	153.18	141.80	64.30	44.22	43.16
	A-HTPGM (80%)	160.63	152.23	141.00	60.74	41.68	39.72
	A-HTPGM (60%)	160.41	151.37	140.66	49.15	40.93	38.05
	A-HTPGM (40%)	156.34	145.96	136.98	46.59	39.64	36.82
	A-HTPGM (20%)	<b>150.24</b>	<b>131.12</b>	<b>128.31</b>	<b>39.03</b>	<b>37.06</b>	<b>30.93</b>

9.5] and 3.69 (TPMiner), [2.8 – 53] and 12.12 (IEMiner), and [3.9 – 56.9] and 16.5 (H-DFS).

The speedups of A-HTPGM compared to E-HTPGM and the baselines depend on the values of  $\mu$ . On tested datasets, the range and average speedups are: [1.1 – 21.3] and 5.2 (E-HTPGM), [3.4 – 203] and 25.1 (TPMiner), [6.4 – 1122] and 115.2 (IEMiner), and [9.3 – 1215] and 230.6 (H-DFS).

It is intuitive that A-HTPGM achieves the highest speedup when  $\mu$  corresponds to the least number of edges in the correlation graph (e.g.,  $\mu = 20\%$ ). However, as shown in Table VII, A-HTPGM obtains similar high speedups when  $\mu = 20\%$ , 40%, and 60%, while also achieving significant speedup with  $\mu = 80\%$ . Moreover, when  $\mu$  is high (e.g.,  $\mu = 60\%$  and 80%),

A-HTPGM also obtains high accuracy (discussed in Section VI-C3). Therefore, we conclude that A-HTPGM can obtain both good performance and high accuracy using high  $\mu$ .

Table VII also shows that A-HTPGM is most effective when the support and confidence thresholds  $\sigma$  and  $\delta$  are low, e.g.,  $\sigma = 20\%$  and  $\delta = 20\%$ . This is because the number of pattern candidates with low support and confidence is large, and thus, it takes a long time to verify all candidates. Using A-HTPGM to prune uncorrelated time series, a majority of such pattern candidates are removed from the mining process.

In average, E-HTPGM consumes 3 times less memory than the baselines due to the applied pruning techniques, while A-HTPGM uses 5 times less memory than E-HTPGM and the

baselines due to the pruning of uncorrelated time series.

Figs. 6 and 7 show an example of the runtime and memory usage of different methods. In this example, data size and the support are fixed ( $\sigma = 20\%$ ), and the confidence changes on the x-axis (y-axis is in log scale in Fig. 6). We can see that A-HTPGM achieves the best performance when the confidence is low, and the gain is not very significant between A-HTPGM and E-HTPGM when the confidence is high.

2) *Evaluation of pruning techniques in E-HTPGM*: We evaluate the runtimes of E-HTPGM to understand how effective the proposed pruning techniques are. We compare different versions of E-HTPGM: (1) E-HTPGM with no pruning, named as NoPrune-E-HTPGM, (2) E-HTPGM with Apriori-based pruning (Lemmas 2, 3), named as Apriori-E-HTPGM, (3) E-HTPGM with transitivity-based pruning (Lemmas 4, 5, 6, 7), named as Trans-E-HTPGM, and (4) E-HTPGM with both pruning techniques applied, named as All-E-HTPGM.

The experiments are run on 3 different configurations: varying the data sizes, varying the confidence, and varying the support. The results are shown in Figs. 8 and 9 (the y-axis is in log scale). It can be seen that All-E-HTPGM achieves the best performance among all versions. Its speedup w.r.t. NoPrune-E-HTPGM ranges from 5 up to 60 depending on the configuration. This shows that the proposed pruning techniques are very effective in improving the performance of E-HTPGM. Furthermore, Apriori-E-HTPGM and Trans-E-HTPGM have different speedups, but the Trans-E-HTPGM is often more efficient than Apriori-E-HTPGM. The average speedup is from 3 to 12 for Apriori-E-HTPGM, and from 8 to 20 for Trans-E-HTPGM. However, applying both prunings always yields better speedup than applying either of them.

3) *Evaluation of A-HTPGM*: In this section, we analyze A-HTPGM from three aspects: (1) the accuracy of A-HTPGM, (2) the quality of patterns pruned by A-HTPGM, and (3) the trade-off between accuracy and runtime gain in A-HTPGM.

First, we compare the patterns extracted by A-HTPGM and E-HTPGM to evaluate the accuracy of A-HTPGM. Table IX shows the results. It can be seen that, A-HTPGM obtains low accuracy when  $\mu$  is low ( $\leq 40\%$ ), relatively high accuracy when  $\mu = 60\%$ , and high accuracy (more than 80% in most cases) when  $\mu \geq 80\%$ . A-HTPGM achieves 100% accuracy (most cases) when  $\mu \geq 90\%$ .

Next, we evaluate the quality of patterns which are pruned by A-HTPGM. These are the patterns extracted from the uncorrelated time series. Fig. 10 shows the cumulative distribution of the confidence computed for the pruned patterns, using  $\mu = 20\%$ . It is seen that the majority of these patterns have low confidences: 80% have confidences less than 20% when the support is 10% and 20%, and 70% of patterns have confidences less than 30% when the support is 30%. These patterns are likely do not satisfy the support and confidence thresholds, and thus can be pruned from the mining process.

Finally, we perform a trade-off analysis between the accuracy and the runtime gain as a means for choosing a proper value of  $\mu$ . In Fig. 11, the accuracy and the runtime gain of A-HTPGM on the tested datasets are plotted together, with  $\mu$

TABLE IX: The accuracy of A-HTPGM

Support (%)	MI $\mu$ (%)	Confidence (%)					
		NIST			Smart City		
		20	50	80	20	50	80
20	40%	52	84	89	48	80	94
	60%	72	85	89	69	81	94
	80%	84	88	100	75	90	99
	90%	99	100	100	100	100	100
50	40%	80	90	100	76	85	96
	60%	87	92	100	80	85	96
	80%	91	94	100	92	96	100
	90%	100	100	100	100	100	100
80	40%	100	100	100	95	95	96
	60%	100	100	100	96	96	96
	80%	100	100	100	100	100	100
	90%	100	100	100	100	100	100

on the x-axis. We can see that, when  $\mu \leq 60\%$ , A-HTPGM obtains significant runtime gain but with low accuracy. However, as  $\mu$  goes beyond 60%, the accuracy increases to 80% while the runtime gain starts decreasing. Based on this trade-off analysis, user can choose a proper value of  $\mu$  depending on her preferences over the performance and accuracy.

4) *Scalability evaluation*: We proceed to evaluate the scalability of E-HTPGM and A-HTPGM on big datasets. First, based on the attributes of NIST, we generate more sequences to create a synthetic dataset that is 5 times bigger than NIST, and similarly for the Smart City dataset. We perform the experiments using two configurations: varying the data sizes (Figs. 12 and 13), and varying the number of attributes (Figs. 14 and 15). We compare the runtimes of A-HTPGM, E-HTPGM and the baselines accordingly.

Figs. 12 and 13 show the runtime comparison when changing the data sizes on NIST and Smart City datasets (y-axis is in log scale). We can see that, A-HTPGM and E-HTPGM scale linearly with the data sizes, with the increasing speed is much lower than the baselines.

When the number of attributes change (Figs. 14 and 15 where y-axis in log scale), the runtimes of A-HTPGM and E-HTPGM increase linearly, while the runtimes of the baselines increase nearly exponential (we can see the straight lines for their runtimes in most cases). Thus, we can conclude that both A-HTPGM and E-HTPGM can scale on big datasets.

## VII. CONCLUSION AND FUTURE WORK

In this paper, we present a comprehensive Frequent Temporal Pattern Mining from Time Series (FTPMfTS) solution that offers: (1) an end-to-end FTPMfTS process to mine frequent temporal patterns from time series, (2) an efficient and exact Hierarchical Temporal Pattern Graph Mining (HTPGM) algorithm that employs efficient data structures and different pruning techniques to achieve fast mining, and (3) an approximate HTPGM that uses mutual information to prune unpromising time series, allows HTPGM to scale on large datasets. The conducted experiments on real-world datasets show that HTPGM outperforms the baselines, and the approximate HTPGM achieves up to 3 orders of magnitude speedup, and scales to large datasets.

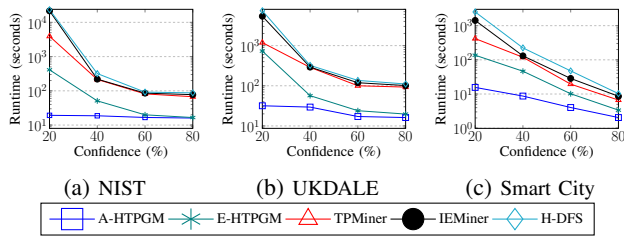


Fig. 6: Runtime comparison

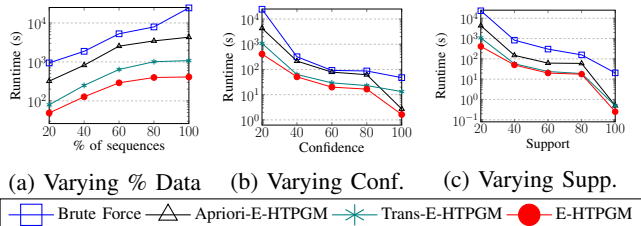


Fig. 8: Runtimes of E-HTPGM on NIST

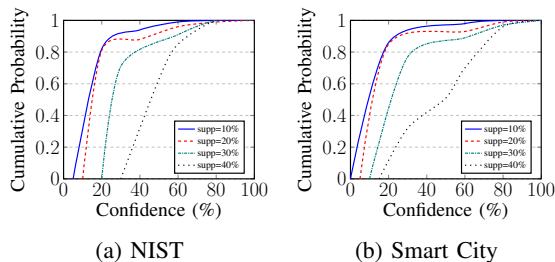


Fig. 10: Cumulative probability of pruned patterns

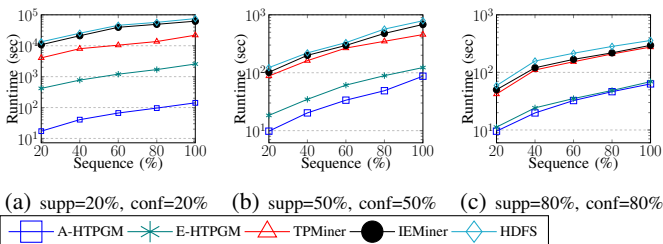


Fig. 12: Scalability test by varying data sizes in NIST

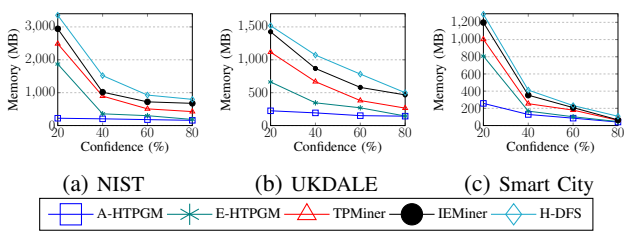


Fig. 7: Memory usage comparison

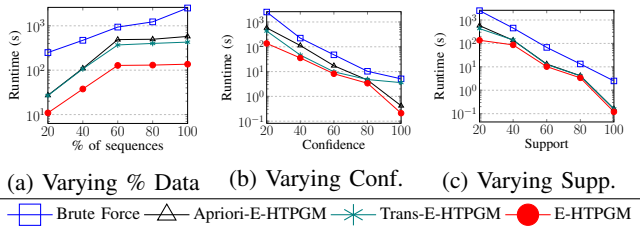


Fig. 9: Runtimes of E-HTPGM on Smart City

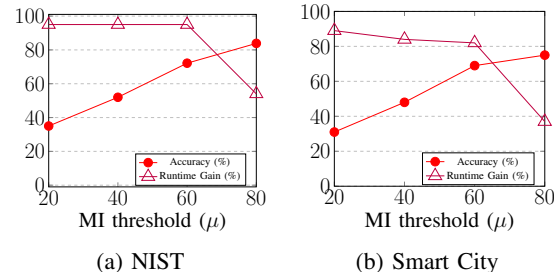


Fig. 11: Trade-off analysis

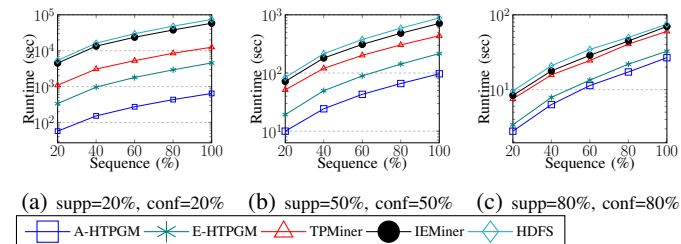


Fig. 13: Scalability test by varying data sizes in Smart City

In future work, we plan to extend HTPGM in order to be able to perform pruning at the attribute level to improve further the performance.

## REFERENCES

- [1] A. U. Ahmed, C. F. Ahmed, M. Samiullah, N. Adnan, and C. K.-S. Leung, "Mining interesting patterns from uncertain databases," *Information Sciences*, vol. 354, 2016.
- [2] J. F. Allen, "Maintaining knowledge about temporal intervals," *Communications of the ACM*, vol. 26, no. 11, pp. 832–843, 1983.
- [3] I. Batal, D. Fradkin, J. Harrison, F. Moerchen, and M. Hauskrecht, "Mining recent temporal patterns for event detection in multivariate time series data," in *SIGKDD*, 2012.
- [4] I. Batal, H. Valizadegan, G. F. Cooper, and M. Hauskrecht, "A temporal pattern mining approach for classifying electronic health record data," *TIST*, vol. 4, 2013.
- [5] J. Blanchard, F. Guillet, R. Gras, and H. Briand, "Using information-theoretic measures to assess association rule interestingness," in *ICDM'05*, 2005.
- [6] E. A. Campbell, E. J. Bass, and A. J. Masino, "Temporal condition pattern mining in large, sparse electronic health record data: A case study in characterizing pediatric asthma," *JAMIA*, vol. 27, 2020.
- [7] Y. Chen, W. Peng, and S. Lee, "Mining temporal patterns in time interval-based data," *TKDE*, vol. 27, no. 12, pp. 3318–3331, 2015.
- [8] N. Y. City. (2019) Nyc opendata. [Online]. Available: <https://opendata.cityofnewyork.us/>
- [9] T. M. Cover and J. A. Thomas, *Elements of Information Theory*. USA: Wiley-Interscience, 1991.
- [10] X. Cunjin, S. Wanjiào, Q. Lijuan, D. Qing, and W. Xiaoyang, "A mutual-information-based mining method for marine abnormal association rules," *Computers & Geosciences*, vol. 76, 2015.
- [11] P. S. Data. (2016) Pecan street dataport. [Online]. Available: <https://www.pecanstreet.org/dataport/>
- [12] W. Healy, A. H. Fanney, B. Dougherty, W. V. Payne, T. Ullah, L. Ng, and F. Omar. (2018) Net zero energy residential test facility instrumented

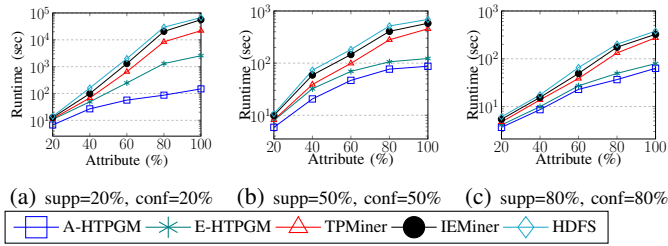


Fig. 14: Scalability test by varying # of attributes in NIST

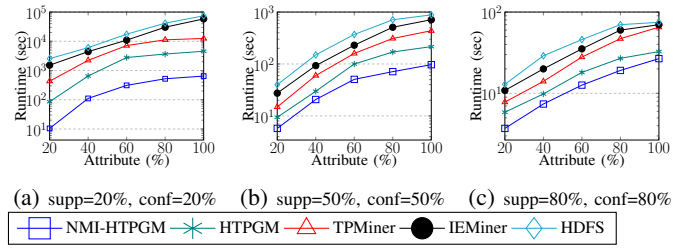


Fig. 15: Scalability test by varying # of attributes in Smart City

data. [Online]. Available: <https://pages.nist.gov/netzero/index.html/>

- [13] V. L. Ho, N. Ho, and T. B. Pedersen, "Efficient temporal pattern mining in big time series using mutual information," *arXiv preprint arXiv:2010.03653*, 2020.
- [14] P.-s. Kam and A. W.-C. Fu, "Discovering temporal patterns for interval-based events," in *DaWak*. Springer, 2000.
- [15] Y. Ke, J. Cheng, and W. Ng, "Correlated pattern mining in quantitative databases," *(TODS, vol. 33, 2008)*.
- [16] J. Kelly and W. Knottenbelt, "The UK-DALE dataset, domestic appliance-level electricity demand and whole-house demand from five UK homes," *Scientific Data*, 2015.
- [17] Y.-K. Lee, W.-Y. Kim, Y. D. Cai, and J. Han, "Comine: Efficient mining of correlated patterns," in *ICDM*, 2003.
- [18] R. Moskovitch and Y. Shahar, "Fast time intervals mining using the transitivity of temporal relations," *KAIS*, vol. 42, 2015.
- [19] D. Nguyen, W. Luo, D. Phung, and S. Venkatesh, "Ltarm: a novel temporal association rule mining method to understand toxicities in a routine cancer treatment," *KBS*, vol. 161, 2018.
- [20] P. Papapetrou, G. Kollios, S. Sclaroff, and D. Gunopulos, "Mining frequent arrangements of temporal intervals," *KAIS*, vol. 21, 2009.
- [21] D. Patel, W. Hsu, and M. L. Lee, "Mining relationships among interval-based events for classification," ser. SIGMOD '08, 2008.
- [22] S.-Y. Wu and Y.-L. Chen, "Mining nonambiguous temporal patterns for interval-based events," *TKDE*, vol. 19, 2007.
- [23] Y. Yao, "Information-theoretic measures for knowledge discovery and data mining," in *Entropy measures, maximum entropy principle and emerging applications*. Springer, 2003, pp. 115–136.

A. Proof of complexity of frequent single event mining

*Complexity:* Let  $m$  be the number of distinct events in  $\mathcal{D}_{\text{SEQ}}$ . The complexity of finding frequent single events is  $O(m \cdot |\mathcal{D}_{\text{SEQ}}|)$ .

*Proof.* Computing the support for each event  $E_i$  takes  $O(|\mathcal{D}_{\text{SEQ}}|)$  (to count the set bits of the *bitmap*  $b_{E_i}$  of length  $|\mathcal{D}_{\text{SEQ}}|$ ). Thus, counting the support for  $m$  events takes  $O(m \cdot |\mathcal{D}_{\text{SEQ}}|)$ .  $\square$

B. Proof of Lemma 1

**Lemma 1.** Let  $m$  be the number of distinct events in  $\mathcal{D}_{\text{SEQ}}$ , and  $h$  be the longest length of a temporal pattern. The total number of temporal patterns in HPG from level  $L_1$  to level  $L_h$  is  $O(m^h 3^{h^2})$ .

*Proof.* At  $L_1$ , the number of nodes is:  $N_1 = m \sim O(m)$ . At  $L_2$ , the number of permutations of  $m$  distinct events taken 2 at a time is:  $P(m, 2)$ . However, since the same event can form a pair of events with itself, e.g., (KOn, KOn), the total number of nodes at  $L_2$  is:  $N_2 = P(m, 2) + m \sim O(m^2)$ . Each node in  $N_2$  can form 3 different temporal relations, and thus, the total number of 2-event patterns in  $L_2$  is:  $N_2 \times 3^1 \sim O(m^2 3^1)$ . Similarly, the number of 3-event nodes at  $L_3$  is:  $N_3 = P(m, 3) + P(m, 2) + m \sim O(m^3)$ , and the number of 3-event patterns is:  $N_3 \times 3^3 \sim O(m^3 3^3)$ . At level  $L_h$ , the number of nodes is  $O(m^h)$ , while the number of  $h$ -event patterns is  $O(m^h \times 3^{\frac{1}{2}h(h-1)}) \sim O(m^h 3^{h^2})$ . Therefore, the total number of temporal patterns from  $L_1$  to  $L_h$  in HPG is  $O(m) + O(m^2 3^1) + O(m^3 3^3) + \dots + O(m^h 3^{h^2}) \sim O(m^h 3^{h^2})$ .  $\square$

C. Proof of complexity of frequent 2-event pattern mining

*Complexity:* Let  $m$  be the number of frequent single events in  $L_1$ , and  $i$  be the average number of instances of each event. The complexity of frequent 2-event pattern mining is  $O(m^2 i^2 |\mathcal{D}_{\text{SEQ}}|^2)$ .

*Proof.* The Cartesian product of  $m$  events in  $L_1$  generates  $m^2$  event pairs. To compute the support of  $m^2$  event pairs, we count the set bits of the *bitmap* that takes  $O(m^2 |\mathcal{D}_{\text{SEQ}}|)$ .

For each node in  $L_2$ , we need to compute the support and confidence of their temporal relations, which takes  $O(i^2 |\mathcal{D}_{\text{SEQ}}|^2)$ . We have potentially  $m^2$  nodes. And thus, it takes  $O(m^2 i^2 |\mathcal{D}_{\text{SEQ}}|^2)$ .

The overall complexity is:  $O(m^2 |\mathcal{D}_{\text{SEQ}}| + m^2 i^2 |\mathcal{D}_{\text{SEQ}}|^2) \sim O(m^2 i^2 |\mathcal{D}_{\text{SEQ}}|^2)$ .  $\square$

D. Proof of Lemma 4.

**Lemma 4** Let  $S = \langle e_1, \dots, e_{n-1} \rangle$  be a temporal sequence that supports an  $(n-1)$ -event pattern  $P = \langle (E_{1 \triangleright e_1}, r_{12}, E_{2 \triangleright e_2}), \dots, (E_{n-2 \triangleright e_{n-2}}, r_{(n-2)(n-1)}, E_{n-1 \triangleright e_{n-1}}) \rangle$ . Let  $e_n$  be an event instance that is combined with  $S$  to create a new temporal sequence  $S' = \langle e_1, \dots, e_n \rangle$ .

Then the set of temporal relations  $\mathfrak{R}$  is transitive on  $S'$ :  $\forall e_i \in S', i \neq n, \exists r \in \mathfrak{R}$  s.t.  $r(E_{i \triangleright e_i}, E_{n \triangleright e_n})$  holds.

*Proof.* Since  $S' = \langle e_1, \dots, e_n \rangle$  is a temporal sequence, the event instances in  $S'$  are chronologically ordered by their start times. Then,  $\forall e_i \in S', i \neq n: t_{s_i} \leq t_{s_n}$ . We have:

- If  $t_{e_i} \pm \epsilon \leq t_{s_n}$ , then  $E_{i \triangleright e_i} \rightarrow E_{n \triangleright e_n}$ .
- If  $(t_{s_i} \leq t_{s_n}) \wedge (t_{e_i} \pm \epsilon \geq t_{e_n})$ , then  $E_{i \triangleright e_i} \succcurlyeq E_{n \triangleright e_n}$ .
- If  $(t_{s_i} < t_{s_n}) \wedge (t_{e_i} \pm \epsilon < t_{e_n}) \wedge (t_{e_i} - t_{s_n} \geq d_o \pm \epsilon)$  where  $d_o$  is the minimal overlapping duration, then  $E_{i \triangleright e_i} \not\bowtie E_{n \triangleright e_n}$ .  $\square$

E. Proof of Lemma 5

**Lemma 5.** Let  $N_{k-1} = (E_1, \dots, E_{k-1})$  be a frequent combination of  $(k-1)$  events, and  $E_k$  be a frequent single event. The combination  $N_k = N_{k-1} \cup E_k$  cannot form any frequent  $k$ -event temporal patterns if  $\nexists E_i \in N_{k-1}, r \in \mathfrak{R}$  s.t.  $r(E_i, E_k)$  is a frequent temporal relation.

*Proof.* Let  $p_k$  be any  $k$ -event pattern formed by  $N_k$ . Then  $p_k$  is a list of  $\frac{1}{2}k(k-1)$  triples  $(E_i, r_{ij}, E_j)$  where each represents a relation  $r(E_i, E_j)$  between two events. In order for  $p_k$  to be frequent, each of the relations in  $p_k$  must be frequent (Defs. 3.11 and 3.15, and Lemma 4). However, since  $\nexists E_i \in N_{k-1}$  such that  $r(E_i, E_k)$  is frequent,  $p_k$  is not frequent.  $\square$

F. Proof of Lemma 7

**Lemma 7.** Consider two temporal patterns  $P$  and  $P'$ . If  $P' \subseteq P$  and  $\frac{\text{supp}(P')}{\max_{1 \leq k \leq |P|} \{\text{supp}(E_k)\}_{E_k \in P}} \leq \delta$ , then  $\text{conf}(P) \leq \delta$ .

*Proof.* We have:

$$\begin{aligned} \text{conf}(P) &= \frac{\text{supp}(P)}{\max_{1 \leq k \leq |P|} \{\text{supp}(E_k)\}} \\ &\leq \frac{\text{supp}(P')}{\max_{1 \leq k \leq |P|} \{\text{supp}(E_k)\}} \leq \delta \end{aligned}$$

$\square$

G. Proof of complexity of frequent  $k$ -event pattern mining

*Complexity:* Let  $r$  be the average number of frequent  $(k-1)$ -event patterns in each node of  $L_{k-1}$ . The complexity of frequent  $k$ -event pattern mining is  $O(|IFreq| \cdot |L_{k-1}| \cdot r \cdot k^2 \cdot |\mathcal{D}_{\text{SEQ}}|)$ .

*Proof.* For each frequent  $(k-1)$ -event pattern of a node in  $L_k$ , we need to compute the support and confidence of  $\frac{1}{2}(k-1)(k-2)$  triples, which takes  $O(\frac{1}{2}(k-1)(k-2)|\mathcal{D}_{\text{SEQ}}|) \sim O(k^2 |\mathcal{D}_{\text{SEQ}}|)$ .

We have  $|IFreq| \times |L_{k-1}|$  nodes in  $L_k$ , each has  $r$  frequent  $(k-1)$ -event patterns. Thus, the total complexity is:  $O(|IFreq| \cdot |L_{k-1}| \cdot r \cdot k^2 \cdot |\mathcal{D}_{\text{SEQ}}|)$ .  $\square$

## H. Proof of Lemma

**Lemma 8.** Let  $\text{supp}(X_1, Y_1)_{\mathcal{D}_{\text{SYB}}}$  be the support of  $(X_1, Y_1)$  in  $\mathcal{D}_{\text{SYB}}$ , and  $\text{supp}(X_1, Y_1)_{\mathcal{D}_{\text{SEQ}}}$  be the support of  $(X_1, Y_1)$  in  $\mathcal{D}_{\text{SEQ}}$ . We have:  $\text{supp}(X_1, Y_1)_{\mathcal{D}_{\text{SYB}}} \leq \text{supp}(X_1, Y_1)_{\mathcal{D}_{\text{SEQ}}}$ .

*Proof.* Recall that when converting  $\mathcal{D}_{\text{SYB}}$  to  $\mathcal{D}_{\text{SEQ}}$ , we divide the symbolic time series in  $\mathcal{D}_{\text{SYB}}$  into equal length temporal sequences. Let  $n$  be the length of each symbolic time series in  $\mathcal{D}_{\text{SYB}}$ , and  $m$  be the length of each temporal sequence. The number of temporal sequences obtained in  $\mathcal{D}_{\text{SEQ}}$  is:  $\lceil \frac{n}{m} \rceil$ .

The support of  $(X_1, Y_1)$  in  $\mathcal{D}_{\text{SYB}}$  is computed as:

$$\text{supp}(X_1, Y_1)_{\mathcal{D}_{\text{SYB}}} = \frac{\sum_{i=1}^{\lceil \frac{n}{m} \rceil} \sum_{j=1}^m s_{ij}}{n} \quad (12)$$

where

$$s_{ij} = \begin{cases} 1, & \text{if } (X_1, Y_1) \text{ occurs in row } j \text{ of the sequence } s_i \text{ in } \mathcal{D}_{\text{SYB}} \\ 0, & \text{otherwise} \end{cases}$$

Intuitively, Eq. 12 computes the relative support of  $(X_1, Y_1)$  in  $\mathcal{D}_{\text{SYB}}$  by counting the number of times  $(X_1, Y_1)$  occurs in  $\mathcal{D}_{\text{SYB}}$ , and then dividing to the size of  $\mathcal{D}_{\text{SYB}}$ .

On the other hand, the support of  $(X_1, Y_1)$  in  $\mathcal{D}_{\text{SEQ}}$  is computed by counting the number of sequences in  $\mathcal{D}_{\text{SEQ}}$  that  $(X_1, Y_1)$  occurs. Note that if  $(X_1, Y_1)$  occurs more than one in the same sequence, we will count only 1 for that sequence. Thus, we have:

$$\text{supp}(X_1, Y_1)_{\mathcal{D}_{\text{SEQ}}} = \frac{\sum_{i=1}^{\lceil \frac{n}{m} \rceil} g_i}{n/m} = \frac{m \cdot \sum_{i=1}^{\lceil \frac{n}{m} \rceil} g_i}{n} \quad (13)$$

where

$$g_i = \begin{cases} 1, & \text{if } (X_1, Y_1) \text{ occurs in the sequence } g_i \text{ in } \mathcal{D}_{\text{SEQ}} \\ 0, & \text{otherwise} \end{cases}$$

Compare Eqs. 12 and 13, we have:

$$\sum_{i=1}^{\lceil \frac{n}{m} \rceil} \sum_{j=1}^m s_{ij} \leq m \cdot \sum_{i=1}^{\lceil \frac{n}{m} \rceil} g_i \quad (14)$$

Hence:

$$\text{supp}(X_1, Y_1)_{\mathcal{D}_{\text{SYB}}} \leq \text{supp}(X_1, Y_1)_{\mathcal{D}_{\text{SEQ}}} \quad (15)$$

□

## I. Proof of Theorem

**Theorem 1.** Let  $\sigma$ ,  $\sigma_m$  be the minimum and maximum support thresholds,  $\mu$  be the mutual information threshold. Assume that  $(X_1, Y_1)$  is frequent in  $\mathcal{D}_{\text{SYB}}$ :  $\sigma \leq \text{supp}(X_1, Y_1)_{\mathcal{D}_{\text{SYB}}} \leq \sigma_m$ .

If the normalized mutual information  $\tilde{I}(\mathcal{X}_S; \mathcal{Y}_S) \geq \mu$ , then the confidence of the event pair  $(X_1, Y_1)$  in  $\mathcal{D}_{\text{SEQ}}$  has a lower bound LB:

$$\text{conf}(X_1, Y_1)_{\mathcal{D}_{\text{SEQ}}} \geq \text{LB where:} \\ \text{LB} = \left( \sigma^{\sigma_m} \cdot \left( \frac{1 - \sigma_m}{n_x - 1} \right)^{1 - \sigma} \right)^{\frac{1 - \mu}{\sigma}} \cdot \frac{\sigma}{2 \cdot \sigma_m - \sigma} \quad (16)$$

where  $n_x$  is the number of symbols in the symbol alphabet  $\Sigma_X$ .

*Proof.* From Eq. (10), we have:

$$\tilde{I}(\mathcal{X}_S; \mathcal{Y}_S) = 1 - \frac{H(\mathcal{X}_S | \mathcal{Y}_S)}{H(\mathcal{X}_S)} \geq \mu \quad (17)$$

Hence:

$$\frac{H(\mathcal{X}_S | \mathcal{Y}_S)}{H(\mathcal{X}_S)} \leq 1 - \mu \quad (18)$$

First, we derive a lower bound for  $\frac{H(\mathcal{X}_S | \mathcal{Y}_S)}{H(\mathcal{X}_S)}$ .

$$\begin{aligned} \frac{H(\mathcal{X}_S | \mathcal{Y}_S)}{H(\mathcal{X}_S)} &= \frac{p(X_1, Y_1) \cdot \log p(X_1 | Y_1)}{p(X_1) \cdot \log p(X_1) + \sum_{i \neq 1} p(X_i) \cdot \log p(X_i)} \\ &+ \frac{\sum_{i \neq 1 \& j \neq 1} p(X_i, Y_j) \cdot \log \frac{p(X_i, Y_j)}{p(Y_j)}}{p(X_1) \cdot \log p(X_1) + \sum_{i \neq 1} p(X_i) \cdot \log p(X_i)} \end{aligned} \quad (19)$$

Applying the log sum inequality [9] for the second term of the denominator in Eq. (19), we get:

$$\begin{aligned} \sum_{i \neq 1} p(X_i) \cdot \log p(X_i) &\geq \sum_{i \neq 1} p(X_i) \log \frac{\sum_{i \neq 1} p(X_i)}{\sum_{i \neq 1} 1} \quad (20) \\ &= (1 - p(X_1)) \cdot \log \frac{1 - p(X_1)}{n_x - 1} \quad (21) \end{aligned}$$

Replace Eq. (21) into Eq. (19), we get:

$$\frac{H(\mathcal{X}_S | \mathcal{Y}_S)}{H(\mathcal{X}_S)} \geq \frac{p(X_1, Y_1) \cdot \log p(X_1 | Y_1)}{p(X_1) \cdot \log p(X_1) + (1 - p(X_1)) \cdot \log \frac{1 - p(X_1)}{n_x - 1}} \quad (22)$$

\* **Case 1:** Assuming that  $\text{supp}(Y_1)_{\mathcal{D}_{\text{SYB}}} \geq \text{supp}(X_1)_{\mathcal{D}_{\text{SYB}}}$ . Thus, the confidence of  $(X_1, Y_1)$  in  $\mathcal{D}_{\text{SYB}}$  is computed as

$$\text{conf}(X_1, Y_1)_{\mathcal{D}_{\text{SYB}}} = \frac{\text{supp}(X_1, Y_1)_{\mathcal{D}_{\text{SYB}}}}{\text{supp}(Y_1)_{\mathcal{D}_{\text{SYB}}}} = \frac{p(X_1, Y_1)}{p(Y_1)} \quad (23)$$

Since we have:  $\log \frac{p(X_1, Y_1)}{p(Y_1)} < 0$ , and  $\sigma \leq p(X_1, Y_1)$ , we can deduce:

$$p(X_1, Y_1) \cdot \log \frac{p(X_1, Y_1)}{p(Y_1)} \leq \sigma \cdot \log \frac{p(X_1, Y_1)}{p(Y_1)} \quad (24)$$

We also have:  $\log \sigma \leq \log p(X_1) < 0$ , and  $p(X_1) \leq \sigma_m$ , hence:

$$p(X_1) \cdot \log p(X_1) \geq \sigma_m \cdot \log \sigma \quad (25)$$

We also get:  $\log \frac{1 - \sigma_m}{n_x - 1} \leq \log \frac{1 - p(X_1)}{n_x - 1} < 0$ , and  $(1 - p(X_1)) \leq (1 - \sigma)$ , hence:

$$(1 - p(X_1)) \cdot \log \frac{1 - p(X_1)}{n_x - 1} \geq (1 - \sigma) \cdot \log \frac{1 - \sigma_m}{n_x - 1} \quad (26)$$

From Eqs. (25), (26), we have:

$$\begin{aligned} p(X_1) \cdot \log p(X_1) + (1 - p(X_1)) \cdot \log \frac{1 - p(X_1)}{n_x - 1} &\geq \\ \sigma_m \cdot \log \sigma + (1 - \sigma) \cdot \log \frac{1 - \sigma_m}{n_x - 1} \end{aligned} \quad (27)$$

Replace Eq. (24) into the numerator, and Eq. (27) into the denominator of Eq. (22), we get:

$$\frac{H(\mathcal{X}_S|\mathcal{Y}_S)}{H(\mathcal{X}_S)} \geq \frac{\sigma \cdot \log \frac{p(X_1, Y_1)}{p(Y_1)}}{\sigma_m \cdot \log \sigma + (1 - \sigma) \cdot \log \frac{1 - \sigma_m}{n_x - 1}} \quad (28)$$

From Eqs. (18) and (28), it follows that:

$$(1 - \mu) \geq \frac{\sigma \cdot \log \frac{p(X_1, Y_1)}{p(Y_1)}}{\sigma_m \cdot \log \sigma + (1 - \sigma) \cdot \log \frac{1 - \sigma_m}{n_x - 1}} \quad (29)$$

$$\Rightarrow \text{conf}(X_1, Y_1)_{\mathcal{D}_{\text{SYB}}} = \frac{p(X_1, Y_1)}{p(Y_1)} \quad (30)$$

$$\geq \left( \sigma^{\sigma_m} \cdot \left( \frac{1 - \sigma_m}{n_x - 1} \right)^{1 - \sigma} \right)^{\frac{1 - \mu}{\sigma}} \quad (31)$$

\* **Case 2:** Assuming that  $\text{supp}(Y_1)_{\mathcal{D}_{\text{SYB}}} < \text{supp}(X_1)_{\mathcal{D}_{\text{SYB}}}$ . Thus, the confidence of  $(X_1, Y_1)$  in  $\mathcal{D}_{\text{SYB}}$  is computed as

$$\text{conf}(X_1, Y_1)_{\mathcal{D}_{\text{SYB}}} = \frac{p(X_1, Y_1)}{p(X_1)} \quad (32)$$

From Eq. (22), we have:

$$\frac{H(\mathcal{X}_S|\mathcal{Y}_S)}{H(\mathcal{X}_S)} \geq \frac{p(X_1, Y_1) \cdot \log \left( \frac{p(X_1, Y_1)}{p(X_1)} \cdot \frac{p(X_1)}{p(Y_1)} \right)}{p(X_1) \cdot \log p(X_1) + (1 - p(X_1)) \cdot \log \frac{1 - p(X_1)}{n_x - 1}} \quad (33)$$

$$\geq \frac{\sigma \cdot \log \left( \frac{p(X_1, Y_1)}{p(X_1)} \cdot \frac{\sigma_m}{\sigma} \right)}{\sigma_m \cdot \log \sigma + (1 - \sigma) \cdot \log \frac{1 - \sigma_m}{n_x - 1}} \quad (34)$$

From Eqs. (18), (34), it follows that:

$$(1 - \mu) \geq \frac{\sigma \cdot \log \left( \frac{p(X_1, Y_1)}{p(X_1)} \cdot \frac{\sigma_m}{\sigma} \right)}{\sigma_m \cdot \log \sigma + (1 - \sigma) \cdot \log \frac{1 - \sigma_m}{n_x - 1}} \quad (35)$$

$$\Rightarrow \text{conf}(X_1, Y_1)_{\mathcal{D}_{\text{SYB}}} = \frac{p(X_1, Y_1)}{p(X_1)} \quad (36)$$

$$\geq \left( \sigma^{\sigma_m} \cdot \left( \frac{1 - \sigma_m}{n_x - 1} \right)^{1 - \sigma} \right)^{\frac{1 - \mu}{\sigma}} \cdot \left( \frac{\sigma}{\sigma_m} \right) \quad (37)$$

In Eq. (37), we have  $\frac{\sigma}{\sigma_m} < 1$ . Thus, from Eqs. (31), (37), we have the confidence lower bound of  $(X_1, Y_1)$  in  $\mathcal{D}_{\text{SYB}}$  in both cases is:

$$\text{conf}(X_1, Y_1)_{\mathcal{D}_{\text{SYB}}} \geq \left( \sigma^{\sigma_m} \cdot \left( \frac{1 - \sigma_m}{n_x - 1} \right)^{1 - \sigma} \right)^{\frac{1 - \mu}{\sigma}} \quad (38)$$

Next, we consider the confidence of  $(X_1, Y_1)$  in the temporal sequence database  $\mathcal{D}_{\text{SEQ}}$ . From Lemma 8, we have:

$$\text{supp}(X_1)_{\mathcal{D}_{\text{SYB}}} \leq \text{supp}(X_1)_{\mathcal{D}_{\text{SEQ}}} \leq \sigma_m \quad (39)$$

$$\Rightarrow \text{supp}(X_1)_{\mathcal{D}_{\text{SYB}}} + \beta_1 \leq \sigma_m \quad (40)$$

$$\Rightarrow \beta_1 \leq \sigma_m - \sigma \quad (41)$$

where  $\beta_1$  is a non-negative number, and  $\text{supp}(X_1)_{\mathcal{D}_{\text{SYB}}} \geq \sigma$ . Without loss of generality, we assume that  $\text{supp}(X_1)_{\mathcal{D}_{\text{SEQ}}} \geq \text{supp}(Y_1)_{\mathcal{D}_{\text{SEQ}}}$ . Thus, the confidence of  $(X_1, Y_1)$  in  $\mathcal{D}_{\text{SEQ}}$  is computed as

$$\text{conf}(X_1, Y_1)_{\mathcal{D}_{\text{SEQ}}} = \frac{\text{supp}(X_1, Y_1)_{\mathcal{D}_{\text{SEQ}}}}{\text{supp}(X_1)_{\mathcal{D}_{\text{SEQ}}}} \geq \frac{\text{supp}(X_1, Y_1)_{\mathcal{D}_{\text{SYB}}}}{\text{supp}(X_1)_{\mathcal{D}_{\text{SYB}}} + \beta_2} \quad (42)$$

From Eqs. (41), (42), we have:

$$\text{conf}(X_1, Y_1)_{\mathcal{D}_{\text{SEQ}}} \geq \frac{\text{supp}(X_1, Y_1)_{\mathcal{D}_{\text{SYB}}}}{\text{supp}(X_1)_{\mathcal{D}_{\text{SYB}}} + \sigma_m - \sigma} \quad (43)$$

From Eq. 38, we get:

$$\begin{aligned} \text{conf}(X_1, Y_1)_{\mathcal{D}_{\text{SYB}}} &= \frac{\text{supp}(X_1, Y_1)_{\mathcal{D}_{\text{SYB}}}}{\text{supp}(X_1)_{\mathcal{D}_{\text{SYB}}}} \\ &\geq \left( \sigma^{\sigma_m} \cdot \left( \frac{1 - \sigma_m}{n_x - 1} \right)^{1 - \sigma} \right)^{\frac{1 - \mu}{\sigma}} \end{aligned} \quad (44)$$

Let:

$$l = \left( \sigma^{\sigma_m} \cdot \left( \frac{1 - \sigma_m}{n_x - 1} \right)^{1 - \sigma} \right)^{\frac{1 - \mu}{\sigma}} \quad (45)$$

From Eqs. (43), (44), (45), we have:

$$\begin{aligned} \frac{\text{supp}(X_1, Y_1)_{\mathcal{D}_{\text{SYB}}}}{\text{supp}(X_1)_{\mathcal{D}_{\text{SYB}}} + \sigma_m - \sigma} &\geq \frac{l \cdot \text{supp}(X_1)_{\mathcal{D}_{\text{SYB}}}}{\text{supp}(X_1)_{\mathcal{D}_{\text{SYB}}} + \sigma_m - \sigma} \\ &\geq \frac{l \cdot \sigma}{\sigma_m + \sigma_m - \sigma} = \frac{l \cdot \sigma}{2 \cdot \sigma_m - \sigma} \end{aligned} \quad (46)$$

Finally, from Eqs. (43) and (47), we can conclude:

$$\text{conf}(X_1, Y_1)_{\mathcal{D}_{\text{SEQ}}} \geq \left( \sigma^{\sigma_m} \cdot \left( \frac{1 - \sigma_m}{n_x - 1} \right)^{1 - \sigma} \right)^{\frac{1 - \mu}{\sigma}} \cdot \frac{\sigma}{2 \cdot \sigma_m - \sigma} \quad \square$$